Hadamard-based Soft Decoding for Vector Quantization over Noisy Channels

Mikael Skoglund and Per Hedelin

April 1998

To appear in IEEE Trans. on Information Theory

IR-S3-SB-9818

ROYAL INSTITUTE
OF TECHNOLOGY
Department of
Signals, Sensors & Systems
Signal Processing
S-100 44 STOCKHOLM

KUNGL TEKNISKA HÖGSKOLAN
Institutionen för
Signaler, Sensorer & System
Signalbehandling
100 44 STOCKHOLM

Hadamard-based Soft Decoding for Vector Quantization over Noisy Channels

Mikael Skoglund and Per Hedelin

Submitted January 1996 to
IEEE Transactions on Information Theory

Accepted for publication January 1998
Final version submitted April 3, 1998

Abstract: We present an estimator-based, or soft, vector quantizer decoder for communication over a noisy channel. The decoder is optimal according to the mean-square error criterion, and Hadamard-based in the sense that a Hadamard transform representation of the vector quantizer is utilized in the implementation of the decoder. An efficient algorithm for optimal decoding is derived. We furthermore investigate suboptimal versions of the decoder, providing good performance at lower complexity. The issue of joint encoder–decoder design is considered both for optimal and suboptimal decoding. Results regarding the channel distortion and the structure of a channel robust code are also provided. Through numerical simulations, soft decoding is demonstrated to outperform hard decoding in several aspects.

Index terms: vector quantization, combined source–channel coding, noisy channels, estimation, soft decoding, index assignment.

1 Introduction

Traditionally the source and the channel codes of a communication system are designed and used separately. As is well-known, the separation of the source and the channel coding gives no loss in optimality if infinite complexity (delay) is permitted [1, 2]. However, in practical systems, where delay can be a major obstacle, combined source and channel coding may give advantages over traditional tandem coding. Motivated by this fact, the study of vector quantization (VQ)[1] for noisy channels has become a major field of research [3, 4, 5, 6, 7, 8, 9, 7, 10, 11, 12, 13, 14, 15, 16].

When designing a VQ system for a noisy channel, essentially one can take on one of two approaches. We will refer to these as the robust VQ (RVQ) approach, and the channel optimized VQ (COVQ)

[1] We will use the acronym "VQ" to mean, interchangeably, "vector quantization" and "vector quantizer".

approach. In the first approach, RVQ, the VQ is trained for a noiseless channel and is subsequently made robust against channel errors by the use of an index assignment (IA) algorithm. Index assignment is the procedure of labeling the codevectors of a VQ suitably in order to reduce the impact of channel errors on the reproduction fidelity (c.f., [17, 18, 19]). The RVQ approach gives a system that is inherently robust over a set of channels of various qualities. On the other hand, in the COVQ approach the system is trained for a specific channel, that is, given that the channel is known. Such knowledge modifies the fidelity criterion in the design to take the distortion introduced by the channel into account (see, e.g., [5, 6, 17, 7, 10, 11]).

Most previous work on channel robust VQ has considered discrete channel models with an emphasis on the binary symmetric channel (e.g., [3, 5, 8, 6, 17, 7, 18, 19, 14]). In this paper we depart from this path in that we assume that the VQ decoder can use the soft (unquantized) channel output for decoding. Such an assumption leads in a natural fashion to a decoder that is a minimum mean-square error (MMSE) estimator (c.f., [10, 13]). We will refer to a decoder that uses the analog channel output as a *soft* decoder to distinguish it from a conventional VQ decoder based on a hard decision and a table look-up. The main contribution of this paper is a framework for soft decoding based on a Hadamard transform representation of the VQ. We show that this framework has certain advantages over the more straightforward approach of, e.g., [13].

For clarity, we refer to VQ with soft decoding by an additional suffix "SD" in abbreviations (e.g., VQ-SD, RVQ-SD and COVQ-SD), and to ordinary hard (table look-up) decoding by an additional "HD" (e.g., VQ-HD and COVQ-HD), as was also done in [20].

1.1 Historical survey and related work

The overarching subject of this paper is "vector quantization over a noisy channel". Much present research in this area originates in [5], where criteria for optimality were first formulated. Subsequent landmarks in the development of the subject include [17, 18, 7]. The first two of these concentrate on the IA problem, and [7] investigates the design and structure of COVQs. The first treatment of soft decoding for VQ over a noisy channel can be found in [10]. This work considered a linear approximation to the generally nonlinear MMSE decoder for the AWGN channel. The results of [10] were extended to the nonlinear optimal decoder in [13]. Later work, related to [13] and by the same authors, utilizing the nonlinear decoder on a channel with uncorrelated fading can be found in [21, 22]. Furthermore, an early treatment of soft decoding for trellis coded quantization over the AWGN channel can be found in the thesis [23]. The version of the Hadamard-based soft decoder that is referred to as the full entropy decoder below, was introduced in [20, 24] and was later generalized to the optimal nonlinear case in [25, 26]. An application of the optimal Hadamard-based soft decoder to image transmission can be found in [25], and an application to speech coding in [27].

The Hadamard transform representation of a VQ plays an important role in the present study. It was

first described for VQ-HD in [28], and was further investigated in the thesis [12]. A related framework for construction of constrained VQs having good channel distortion robustness was presented in [14, 29]. Also, the two book chapters [15, 16] provide a thorough treatment of Hadamard methods for VQ-HD analysis.

1.2 Organization of the paper

We begin with a preliminary section stating the problem under consideration and introducing the notation used. Then, in Section 3, we derive and analyze the the Hadamard-based MMSE decoder having the leading role of this paper. Here we also state an algorithm for decoder computations. In Section 4 we handle the special case of decoding for full entropy encoding. Next, in Section 5, we investigate some aspects of system design and present design algorithms. In Section 6, the channel distortion of a system with Hadamard-based soft decoding is analyzed and results concerning the structure of a robust system are given. Finally we present numerical results and comparisons in Section 7. Section 8 is a summary of the paper.

2 Preliminaries

We study block source coding, or vector quantization, over a noisy channel. The investigation is based on the communication system model depicted Figure 1. In the following three sub-sections we describe the basic assumptions made about the different blocks of the system.

2.1 The source and the VQ encoder

We will consider a d-dimensional vector source $\{\mathbf{X}_n\}$ where one source vector is described by the marginal probability density function (pdf) $f_{\mathbf{X}}(\mathbf{x})$. The source is a zero mean, stationary, and ergodic stochastic process. Because of the stationarity of the source, we will omit the specification of the time index n. The

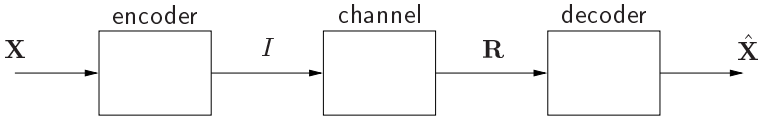

Figure 1: The communication system.

encoder of the block source code is a mapping $\varepsilon : \mathbb{R}^d \to \{0, 1, \ldots, N-1\}$, such that $\varepsilon(\mathbf{X}) = I$ for the source vector $\mathbf{X}$. The mapping of the encoder is described by $\mathbf{X} \in \mathcal{S}_i \Rightarrow I = i$ where $\{\mathcal{S}_i\}_{i=0}^{N-1}$ is a partition of $\mathbb{R}^d$, and where $N = 2^k$ (thus the rate of the source code is $R = k/d$ bits per dimension). The sets $\{\mathcal{S}_i\}$ are called the *encoder regions*. When $I = i$, let $\mathbf{b}_i = (b_1(i), b_2(i), \ldots, b_k(i))^T$, where $b_m(i) \in \{-1, +1\}$, be a vector containing the bits[2] of the index, i. We assume that the bits, $b_m(i)$, are determined by the natural

[2]We will use the term *bit* for the number $b_m(I) \in \{\pm 1\}$, even if this notation is perhaps more common when $b_m(I) \in \{0, 1\}$.

binary code for the index i, replacing logical "zero" with the integer $+1$, and logical "one" with -1. Let $P_i \triangleq \Pr(I = i) = \Pr(\mathbf{X} \in \mathcal{S}_i)$ denote the a-priori probability that index i is chosen by the encoder. The *encoder entropy* is defined as the entropy of the random variable I, $H(I) = -\sum_{i=0}^{N-1} P_i \cdot \log_2 P_i$. In the following we will say that the encoder is a *full entropy encoder*[3] if $P_i = 1/N$, $\forall i$ and, thus, $H(I) = k$ (bits). Decoding for full entropy encoders will be investigated as a special case in Section 4. Finally, for later reference, define the *encoder centroids* $\{\mathbf{c}_i\}_{i=0}^{N-1}$, as $\mathbf{c}_i \triangleq E[\mathbf{X}|I = i] = E[\mathbf{X}|\mathbf{X} \in \mathcal{S}_i]$.

2.2 Channel models

In the most general case we consider, the *channel* is given by an arbitrary pdf, $f_{\mathbf{R}|I}(\mathbf{r}\,|i)$, which describes the stochastic relationship between the transmitted index, I, and the received L-dimensional vector $\mathbf{R}$. We assume that the channel introduces no memory between vectors corresponding to indices transmitted at different times. One common special case of this general channel, is the L-dimensional *additive white Gaussian noise* (AWGN) channel, where the received vector is given by $\mathbf{R} = \mathbf{s}_i + \mathbf{W}$. Here, the transmitted L-dimensional vector $\mathbf{s}_i$ is chosen from a finite set $\{\mathbf{s}_i\}_{i=0}^{N-1}$ of channel symbols, and $\mathbf{W}$ is zero-mean, white and Gaussian; $E[\mathbf{W}\mathbf{W}^T] = \sigma_W^2\mathbf{I}$. ($\mathbf{I}$ denotes the identity matrix.) For this channel we assume, without loss of generality, that the mapping from an input vector, $\mathbf{X}$, to a channel symbol, $\mathbf{s}$, is $\mathbf{s} = \mathbf{s}_{\varepsilon(\mathbf{X})}$. Another important special case is a binary input channel with an unquantized (soft) output. Here, the channel output, R_m, corresponding to the input bit, $b_m(I)$, is

$$R_m = A_m \cdot b_m(I) + W_m, \quad m = 1, 2, ..., k \tag{1}$$

where $\{A_m\}$ describes amplitude variation and the additive noise $\{W_m\}$ is white and zero-mean Gaussian with variance σ_W^2. The received vector, corresponding to one transmitted index I, is $\mathbf{R} = (R_1,\ R_2,\ ...,\ R_k)^T$ (thus the channel dimension is $L = k$, the number of transmitted bits). We refer to a channel described by (1) as an unquantized binary memoryless channel, or just a *binary channel* for convenience. For binary channels, we treat two cases; (*i*) The *known-amplitude binary* (KAB) channel, with $A_m = a$, $\forall m$, and; (*ii*) The *Rayleigh-amplitude binary* (RAB) channel, where $\{A_m\}$ has the marginal pdf $f_A(a) = a/\sigma_A^2 \exp[-a^2/(2\sigma_A^2)]$. We assume the process $\{A_m\}$ to be white, with the physical interpretation of a perfect interleaving in the transmission. The quality of the channel is expressed in terms of the *channel SNR* (CSNR), which is a^2/σ_W^2 for the KAB channel and $E[A_n^2]/\sigma_W^2 = 2\cdot\sigma_A^2/\sigma_W^2$ for the RAB channel. We define the corresponding *hard* binary channels as the binary symmetric channels obtained when taking hard decisions, $\hat{b}_m^{\text{hard}} = \text{sign}(r_m)$, on the soft channel outputs, r_m. The *average bit error rate* (BER), q, for the corresponding hard binary channels is $q = 0.5\cdot\text{erfc}(\sqrt{a^2/2\sigma_W^2})$, where, $\text{erfc}(x) = 2/\sqrt{\pi}\cdot\int_x^\infty \exp(-t^2)dt$, for the KAB channel and $q = 0.5\cdot[1 - \sqrt{\sigma_A^2/(\sigma_A^2 + \sigma_W^2)}]$ for the RAB channel (c.f. [30]). In this paper we

[3]Note that this property depends on the source. Thus a more correct notation would be a full entropy source/encoder *pair*. However, we will refer to the encoder as a full entropy encoder, under the assumption that the encoder is used on the source for which it was designed. See Section 4 for a further discussion.

will emphasize the KAB and the RAB channels since, as will be seen, the Hadamard-based VQ decoder exhibits particularly useful structure for these channels.

2.3 The soft VQ decoder

We study the class of decoders that can be described by vector valued mappings $\delta : \mathbb{R}^L \to \mathbb{R}^d$. The decoder makes use of the channel output, $\mathbf{R}$, and maps it into a source vector estimate $\delta(\mathbf{R})$. We call such decoders *soft decoders* since it is assumed that the decoder can utilize the unquantized (soft) channel output, $\mathbf{R}$. Such decoders can also be referred to as estimator-based (c.f., [10]) contrasting the detector-based decoders that are usually employed in vector quantization. In detector-based decoding the decoder is simply a table look-up based on hard decisions. We also assume that the decoder is a function of the channel output, $\mathbf{R}$, corresponding to *one* transmitted encoder index, I. A more general case is where the decoder regards all channel outputs from time zero (or a subset thereof). This case was studied in [31] for a discrete channel, and in [22] for soft decoding.

By an "optimal" decoder we will throughout refer to optimal in the minimum mean-square error sense. That is, a decoder, δ^*, is optimal if $E\left\|\mathbf{X} - \delta^*(\mathbf{R})\right\|^2 \leq E\left\|\mathbf{X} - \delta(\mathbf{R})\right\|^2$, $\forall\delta$, where δ denotes an arbitrary mapping $\delta : \mathbb{R}^L \to \mathbb{R}^d$. We refer to the mean-square error $D = E\left\|\mathbf{X} - \delta(\mathbf{R})\right\|^2$ as the *distortion* D. Consequently, we will confine the discussion to the class of MMSE soft decoders. The mean-square error is by far the most popular fidelity criterion in vector quantizer design [32] and is well suited for theoretical analysis. The structure of the optimal decoder will be investigated next.

3 The Hadamard-Based Optimal Decoder

In this section we study an implementation of the optimal decoder. The decoder is expressed in terms of a Hadamard framework. This Hadamard formulation of the optimal decoder is the main contribution of this paper. In deriving the optimal decoder we assume that the encoder (as defined by the encoder regions, $\{\mathcal{S}_i\}$) is known and fixed.

3.1 Decoder structure

From estimation theory we know that the decoder function, δ, that minimizes the distortion D can be written as the conditional expected value

$$\delta^*(\mathbf{r}) = E[\mathbf{X}|\,\mathbf{R} = \mathbf{r}]. \tag{2}$$

In [10] a linear approximation to (2) was studied. The results of [10] were later generalized in [13] where the generally nonlinear MMSE decoder of (2) was investigated. The conditional expectation of (2) can be expressed in terms of the conditional pdf, $f_{\mathbf{X}|\mathbf{R}}(\mathbf{x}|\mathbf{r})$, for the source vector, $\mathbf{X}$, given the channel output, $\mathbf{R}$,

as $E[\mathbf{X}|\mathbf{R}=\mathbf{r}] = \int \mathbf{x}\, f_{\mathbf{X}|\mathbf{R}}(\mathbf{x}|\mathbf{r})d\mathbf{x}$. Since $f_{\mathbf{X}|\mathbf{R}}(\mathbf{x}|\mathbf{r}) = f_{\mathbf{X}}(\mathbf{x})f_{\mathbf{R}|\mathbf{X}}(\mathbf{r}|\mathbf{x})/f_{\mathbf{R}}(\mathbf{r})$ and $f_{\mathbf{R}|\mathbf{X}}(\mathbf{r}|\mathbf{x}) = f_{\mathbf{R}|I}(\mathbf{r}|i)$ when $\mathbf{x} \in \mathcal{S}_i$, (2) can be rewritten

$$\begin{aligned} E[\mathbf{X}|\mathbf{R}=\mathbf{r}] &= \sum_{i=0}^{N-1} \int_{\mathcal{S}_i} \mathbf{x} \cdot \frac{f_{\mathbf{R}|I}(\mathbf{r}|i)f_{\mathbf{X}}(\mathbf{x})}{f_{\mathbf{R}}(\mathbf{r})} d\mathbf{x} = \sum_{i=0}^{N-1} \frac{f_{\mathbf{R}|I}(\mathbf{r}|i)P_i}{f_{\mathbf{R}}(\mathbf{r})} \int_{\mathcal{S}_i} \mathbf{x} \cdot f_{\mathbf{X}|I}(\mathbf{x}|i)d\mathbf{x} \\ &= \sum_{i=0}^{N-1} \Pr(I=i|\mathbf{R}=\mathbf{r}) \cdot E[\mathbf{X}|I=i] = \sum_{i=0}^{N-1} \Pr(I=i|\mathbf{R}=\mathbf{r}) \cdot \mathbf{c}_i. \end{aligned}$$

Consequently, the optimal decoder is the conditional expectation (c.f. also [10] and [13])

$$\delta^*(\mathbf{r}) = \sum_{i=0}^{N-1} \Pr(I=i|\mathbf{R}=\mathbf{r}) \cdot \mathbf{c}_i = E[\mathbf{c}_I|\mathbf{R}=\mathbf{r}]. \tag{3}$$

Note that the soft estimate, $\delta^*(\mathbf{r})$, is formed as a convex combination of encoder centroids, and that the set of all possible source vector estimates is a subset of the convex hull of the set of encoder centroids. The treatment of optimal decoding is based on (3). As will be illustrated, the Hadamard matrix and the related Hadamard transform are useful tools in describing the soft decoder. We refer to the set of analytical tools related to the Hadamard matrix as the *Hadamard framework*. As we will see, the Hadamard framework is useful since it provides a description of the optimal source vector estimate in terms of estimates of the individual bits of the transmitted index. We say that a decoder is *Hadamard-based* when it is expressed in the Hadamard framework, while, on the other hand, we refer to (3) as the *general form* of the soft MMSE decoder. The basics of the Hadamard framework is described in Appendix A.

We take the first step in the description of the Hadamard-based decoder by expressing the ith encoder centroid as $\mathbf{c}_i = \mathbf{T}\mathbf{h}_i$ where $\mathbf{h}_i$ is the ith column of an N by N Sylvester-type Hadamard matrix $\mathbf{H}$ (see Appendix A). The *Hadamard column* $\mathbf{h}_i = [h_0(i), \ldots, h_{N-1}(i)]^T$ can (by definition) be expressed in terms of the bits, $b_l(i) \in \{\pm 1\}$, of the index, i, as

$$\mathbf{h}_i = \begin{bmatrix} 1 \\ b_k(i) \end{bmatrix} \otimes \cdots \otimes \begin{bmatrix} 1 \\ b_1(i) \end{bmatrix} = [1,\ b_1(i),\ b_2(i),\ b_1(i)b_2(i),\ \ldots,\ b_1(i)b_2(i)\cdots b_k(i)]^T \tag{4}$$

where $\otimes$ denotes the Kronecker matrix product. Thus, the expression $\mathbf{c}_i = \mathbf{T}\mathbf{h}_i$ gives an explicit relationship between the bits if the index i and the encoder centroid, $\mathbf{c}_i$. The matrix $\mathbf{T}$, the *encoder matrix*, is fully specified by the encoder centroids. By utilizing $\mathbf{c}_i = \mathbf{T}\mathbf{h}_i$ we see that the optimal decoder, δ^*, can be written $\delta^*(\mathbf{r}) = \mathbf{T} \cdot E[\mathbf{h}_I|\mathbf{R}=\mathbf{r}]$. Define $\hat{\mathbf{h}}(\mathbf{r}) \triangleq E[\mathbf{h}_I|\mathbf{R}=\mathbf{r}]$, that is

$$\hat{\mathbf{h}}(\mathbf{r}) = \sum_{i=0}^{N-1} \Pr(I=i|\mathbf{R}=\mathbf{r}) \cdot \mathbf{h}_i = \frac{\sum_{i=0}^{N-1} \mathbf{h}_i P_i f_{\mathbf{R}|I}(\mathbf{r}|i)}{\sum_{j=0}^{N-1} P_j f_{\mathbf{R}|I}(\mathbf{r}|j)}. \tag{5}$$

This quantity is an estimate of the Hadamard column corresponding to the encoder region that was

chosen by the encoder. The estimate, $\hat{\mathbf{h}}(\mathbf{r})$, is referred to as the *soft Hadamard column* in the following. For later reference, let the components of $\hat{\mathbf{h}}(\mathbf{r})$ be denoted as[4] $\hat{h}_n = \hat{h}_n(\mathbf{r}),\ n = 0, 1, \ldots, N-1$.

It is easy to show that the Hadamard columns are orthogonal; $\mathbf{h}_n^T \mathbf{h}_m = \delta_{nm} \cdot N$ (where δ_{nm} denotes the Kronecker delta-function). Consequently, we may write[5]

$$\hat{\mathbf{h}}(\mathbf{r}) = \frac{\sum_{i=0}^{N-1} \mathbf{h}_i P_i f_{\mathbf{R}|I}(\mathbf{r}|i)}{\sum_{j=0}^{N-1} P_j f_{\mathbf{R}|I}(\mathbf{r}|j)} = \frac{\sum_{i=0}^{N-1} P_i \mathbf{h}_i \mathbf{h}_i^T N^{-1} \sum_{n=0}^{N-1} \mathbf{h}_n f_{\mathbf{R}|I}(\mathbf{r}|n)}{\sum_{j=0}^{N-1} P_j \mathbf{h}_j N^{-1} \sum_{m=0}^{N-1} \mathbf{h}_m f_{\mathbf{R}|I}(\mathbf{r}|m)}. \tag{6}$$

To continue, let $\mathbf{R_{hh}} \triangleq \sum_{i=0}^{N-1} P_i \mathbf{h}_i \mathbf{h}_i^T$ and $\mathbf{m_h} \triangleq \sum_{i=0}^{N-1} P_i \mathbf{h}_i$. Also let $\hat{\mathbf{p}}(\mathbf{r}) \triangleq E[\mathbf{h}_I | \mathbf{R} = \mathbf{r}; P_i = 1/N, \forall i]$. Note that $\hat{\mathbf{p}}(\mathbf{r})$ is the a-posteriori expectation of $\mathbf{h}_I$ conditioned on full encoder entropy. Now, since $N^{-1} \sum_{n=0}^{N-1} \mathbf{h}_n f_{\mathbf{R}|I}(\mathbf{r}|n) = [N^{-1} \sum_{i=0}^{N-1} f_{\mathbf{R}|I}(\mathbf{r}|i)] \cdot \hat{\mathbf{p}}(\mathbf{r})$, we have, using (6) and canceling common terms, that $\hat{\mathbf{h}}(\mathbf{r}) = [\mathbf{m}_\mathbf{h}^T \cdot \hat{\mathbf{p}}(\mathbf{r})]^{-1} \mathbf{R_{hh}} \cdot \hat{\mathbf{p}}(\mathbf{r})$. Note that in this expression for $\hat{\mathbf{h}}(\mathbf{r})$ the a-priori information, stemming from the source statistics, is contained in the entities $\mathbf{R_{hh}}$ and $\mathbf{m_h}$, and that the structure of $\hat{\mathbf{p}}(\mathbf{r})$ depends on the channel only. We summarize the above results in the following theorem:

Theorem 1 (The Hadamard-based soft decoder) *Let the encoder centroids be given as $\mathbf{c}_i = \mathbf{T}\mathbf{h}_i$, $i = 0, 1, \ldots, N-1$, where $\mathbf{h}_i$ is the ith Hadamard column (4). Consider a general channel described by $f_{\mathbf{R}|I}(\mathbf{r}|i)$. Over this channel the MMSE decoder, $\delta^*(\mathbf{r})$, can be expressed as $\delta^*(\mathbf{r}) = \hat{\mathbf{X}}(\mathbf{r})$ where*

$$\hat{\mathbf{X}}(\mathbf{r}) \triangleq \mathbf{T}\hat{\mathbf{h}}(\mathbf{r}) \tag{7}$$

and

$$\hat{\mathbf{h}}(\mathbf{r}) = \frac{\mathbf{R_{hh}} \cdot \hat{\mathbf{p}}(\mathbf{r})}{\mathbf{m}_\mathbf{h}^T \cdot \hat{\mathbf{p}}(\mathbf{r})}. \tag{8}$$

The statistic $\hat{\mathbf{p}}(\mathbf{r})$ is defined as

$$\hat{\mathbf{p}}(\mathbf{r}) = E[\mathbf{h}_I | \mathbf{R} = \mathbf{r}; P_i = 1/N, \forall i]. \tag{9}$$

The a-priori index probability information is separated from $\hat{\mathbf{p}}(\mathbf{r})$ and is confined to $\mathbf{R_{hh}} = \sum_{i=0}^{N-1} P_i \mathbf{h}_i \mathbf{h}_i^T$ and $\mathbf{m_h} = \sum_{i=0}^{N-1} P_i \mathbf{h}_i$.

The explicit form of the decoder expression depends on the channel model used. As a first, reasonably general, example consider the L-dimensional AWGN channel. Note that a useful characterization of this channel is obtained when expressing the channel symbols in the Hadamard-framework (c.f., Appendix A). That is, $\mathbf{s}_i = \mathbf{K}\mathbf{h}_i$ where $\mathbf{K} \in \mathbb{R}^{L \times N}$ is the transform matrix associated with the channel signals. Then we get an explicit relationship between the bits, $b_n(i)$, of the encoder index i, the corresponding encoder

[4] Generally, throughout the paper, we will also use the notation $\{\mathbf{a}\}_n$ and $\{\mathbf{A}\}_{n,m}$ for the elements of the vector $\mathbf{a}$ and the matrix $\mathbf{A}$, respectively. Unless otherwise stated 0 is the lowest index ($n = 0, 1, 2, \ldots,\ m = 0, 1, 2, \ldots$)

[5] Note that we have e.g. that $(\sum_i P_i \mathbf{h}_i \mathbf{h}_i^T) \sum_n N^{-1} \mathbf{h}_n f_{\mathbf{R}|I}(\mathbf{r}|n) = \sum_{i,n} (N^{-1} P_i \mathbf{h}_i) \mathbf{h}_i^T \mathbf{h}_n f_{\mathbf{R}|I}(\mathbf{r}|n) = \sum_{i,n} N^{-1} P_i \mathbf{h}_i \cdot N\delta_{in} \cdot f_{\mathbf{R}|I}(\mathbf{r}|n) = \sum_i P_i \mathbf{h}_i f_{\mathbf{R}|I}(\mathbf{r}|i)$.

centroid $\mathbf{c}_i = \mathbf{T}\mathbf{h}_i$ and the channel symbol $\mathbf{s}_i = \mathbf{K}\mathbf{h}_i$. Using such a representation for the channel and the encoder centroids, the following result is proved in Appendix B.

Theorem 2 (The L-dimensional AWGN channel) *Consider the L-dimensional AWGN channel,* $\mathbf{R} = \mathbf{s}_i + \mathbf{W}$. *Let the signals be given as* $\mathbf{s}_i = \mathbf{K}\mathbf{h}_i$, *where* $\mathbf{K} \in \mathbb{R}^{L\times N}$ *is a transform matrix. Similarly, let* $||\mathbf{s}_i||^2 = \mathbf{g}^T\mathbf{h}_i$ *where* $\mathbf{g}$ *is a transform vector. Furthermore, let the matrix* $\mathbf{F} \in \mathbb{R}^{2^N\times N}$ *be defined by the equations*

$$\begin{bmatrix} 1 \\ h_{N-1}(i) \end{bmatrix} \otimes \begin{bmatrix} 1 \\ h_{N-2}(i) \end{bmatrix} \otimes \cdots \otimes \begin{bmatrix} 1 \\ h_0(i) \end{bmatrix} = \mathbf{F}\mathbf{h}_i, \quad i = 0, 1, \ldots, N-1. \tag{10}$$

Then

$$\hat{\mathbf{p}}(\mathbf{r}) = \frac{\mathbf{F}^T\mathbf{q}(\mathbf{r})}{\{\mathbf{F}^T\mathbf{q}(\mathbf{r})\}_0} \tag{11}$$

where

$$\mathbf{q}(\mathbf{r}) = \begin{bmatrix} 1 \\ \tanh(r'_{N-1}/(2\sigma_W^2)) \end{bmatrix} \otimes \begin{bmatrix} 1 \\ \tanh(r'_{N-2}/(2\sigma_W^2)) \end{bmatrix} \otimes \cdots \otimes \begin{bmatrix} 1 \\ \tanh(r'_0/(2\sigma_W^2)) \end{bmatrix} \tag{12}$$

with $r'_l = \{2\mathbf{K}^T\mathbf{r} - \mathbf{g}\}_l$. *Hence, the Hadamard-based optimal decoder can be expressed as* $\hat{\mathbf{X}}(\mathbf{r}) = \mathbf{T}\cdot\hat{\mathbf{h}}(\mathbf{r})$ *where*

$$\hat{\mathbf{h}}(\mathbf{r}) = \frac{\mathbf{R}_{\mathbf{hh}}\cdot\mathbf{F}^T\mathbf{q}(\mathbf{r})}{\mathbf{m}_{\mathbf{h}}^T\cdot\mathbf{F}^T\mathbf{q}(\mathbf{r})}. \tag{13}$$

Proof of Theorem 2. See Appendix B.

The matrix $\mathbf{F}$ is well defined, since all elements of the vector in the left-hand side of (10) are also elements of $\mathbf{h}_i$. Consequently, $\mathbf{F}$ has exactly one non-zero element, the number +1, in each row. Thus, the elements of $\tilde{\mathbf{q}}(\mathbf{r}) \triangleq \mathbf{F}^T\mathbf{q}(\mathbf{r})$ are sums of elements from the vector $\mathbf{q}(\mathbf{r})$ which are real numbers in the interval $(-1, +1)$. Note, however, that using $\tilde{\mathbf{q}}(\mathbf{r})$ directly as a basis for decoding is impractical, since $\mathbf{F}$ is a matrix of size $2^N \times N$ and thus of exponential size in N. On the other hand, since the component $\{\tilde{\mathbf{q}}(\mathbf{r})\}_n$ is formed as a sum of elements taken from $\mathbf{q}(\mathbf{r})$, only the *positions* of these elements have to be stored (for each n). Each such sum will consist of relatively few terms. Also, given $\{\tanh(r'_l/(2\sigma_W^2))\}_{l=0}^{N-1}$ an arbitrary element in $\mathbf{q}(\mathbf{r})$ can be computed using less than N multiplications. Thus, generally $\tilde{\mathbf{q}}(\mathbf{r})$ can be computed much more efficiently than a first glance at Theorem 2 suggests[6]. Once $\tilde{\mathbf{q}}(\mathbf{r})$ is known $\hat{\mathbf{h}}(\mathbf{r})$ can be computed using an order of $N\cdot\log N$ operations (see Section 3.3 below).

Without further specification of the channel symbols, $\mathbf{s}_i = \mathbf{K}\mathbf{h}_i$, it is hard to give Theorem 2 an

[6]Note also that the calculation can be performed without storing $\mathbf{q}(\mathbf{r})$ and $\mathbf{F}$.

intuitive interpretation. One example where the theorem becomes easier to interpret is when; (i) $||\mathbf{s}_i||$ is constant over i, and; (ii) $\mathbf{s}_i = \tilde{\mathbf{K}}\mathbf{b}_i$ for some matrix $\tilde{\mathbf{K}}$ (that is, $\mathbf{s}_i$ depends linearly on the bit-vector $\mathbf{b}_i$). Then Theorem 2 gives

$$\hat{\mathbf{p}}(\mathbf{r}) = \begin{bmatrix} 1 \\ \\ \rho_k \end{bmatrix} \otimes \begin{bmatrix} 1 \\ \\ \rho_{k-1} \end{bmatrix} \otimes \cdots \otimes \begin{bmatrix} 1 \\ \\ \rho_1 \end{bmatrix}$$

where $\rho_l = \rho_l(\mathbf{r}) = \tanh(\{\tilde{\mathbf{K}}^T\mathbf{r}\}_{l-1}/\sigma_W^2)$. Comparing this expression to (4) suggests that ρ_l is a *soft estimate of the bit*, $b_l(I)$. Hence, the decoding is built up from soft bit-estimates, or *soft bits* (c.f. [20]), from to the interval $(-1, +1)$ rather than from "hard" bits belonging to $\{\pm 1\}$, giving the decoder expression (13) an enlightening interpretation in this case. As we will see, the interpretation that soft VQ decoding is based on soft bits is a feature of the binary channels as well[7]. Since the main emphasis in this paper is on the binary channels, we will treat them with some extra care next. However, we emphasize that Theorem 2 holds for a very large class of channels, and that most of the results below, derived assuming a binary channel, can be modified to hold for more general channels as well.

In the rest of the paper we will frequently consider the binary channels (KAB and RAB). The main reason for this is that these channels are specifically straightforward to handle in the Hadamard-framework. To see this, note that since independence[8] allows for splitting the conditional expectation in (9) into products of expectations, we have for the binary channels that

$$\hat{\mathbf{p}}(\mathbf{r}) = \begin{bmatrix} 1 \\ \\ \hat{b}(r_k) \end{bmatrix} \otimes \cdots \otimes \begin{bmatrix} 1 \\ \\ \hat{b}(r_1) \end{bmatrix} = (1, \hat{b}(r_1), \hat{b}(r_2), \hat{b}(r_1)\hat{b}(r_2), \hat{b}(r_3), \ldots, \hat{b}(r_1)\cdots\hat{b}(r_k))^T \qquad (14)$$

where $\hat{b}(r_n) \triangleq E[b_n(I)|R_n = r_n; \Pr(b_n = +1) = 1/2]$ is the MMSE estimate of the bit $b_n(I)$ conditioned on equally likely bit-values. We summarize this result in the following theorem:

Theorem 3 (Binary channels) *For a binary channel the statistic* $\hat{\mathbf{p}}(\mathbf{r})$ *can be formed according to* (14) *in terms of the estimates*

$$\hat{b}(r_n) = E[b_n(I)|R_n = r_n; \Pr(b_n = +1) = 1/2] \qquad (15)$$

of the transmitted bits $b_n(I)$.

We employ Theorem 3 for the two binary channels as follows: First, for the KAB channel it is straightforward to show that, $\hat{b}(r_n) = \tanh(ar_n/\sigma_W^2)$. Consequently we have the following result:

[7] For the KAB channel this is not surprising, since it is a special case of the channel described by (i) and (ii). However, the RAB channel is not. Still, it turns out that the RAB channel fits well into the Hadamard framework for VQ decoding.

[8] Note that $b_k(I), \ldots, b_1(I)$ are statistically independent when conditioning that $P_i = N^{-1}$. Together with the assumption of a memoryless channel, (14) follows.

Corollary 1 (The known-amplitude binary channel) *For the known-amplitude binary channel (with $A_n = a$), we have $\hat{\mathbf{X}}(\mathbf{r}) = \mathbf{T}\hat{\mathbf{h}}(\mathbf{r})$ with $\hat{\mathbf{h}}(\mathbf{r}) = \{\mathbf{m}_\mathbf{h}^T\hat{\mathbf{p}}(\mathbf{r})\}^{-1}\mathbf{R}_{\mathbf{hh}}\hat{\mathbf{p}}(\mathbf{r})$, where $\hat{\mathbf{p}}(\mathbf{r})$ is formed according to* (14)*, using $\hat{b}(r_n) = \tanh(ar_n/\sigma_W^2)$.*

Note that since the KAB channel can be treated as a special case of the L-dimensional AWGN channel, this result also follows from Theorem 2. Similarly, for the RAB channel we have the following corollary:

Corollary 2 (The Rayleigh-amplitude binary channel) *For the Rayleigh-amplitude binary channel we have $\hat{\mathbf{X}}(\mathbf{r}) = \mathbf{T}\hat{\mathbf{h}}(\mathbf{r})$ with $\hat{\mathbf{h}}(\mathbf{r}) = \{\mathbf{m}_\mathbf{h}^T\hat{\mathbf{p}}(\mathbf{r})\}^{-1}\mathbf{R}_{\mathbf{hh}}\hat{\mathbf{p}}(\mathbf{r})$, where $\hat{\mathbf{p}}(\mathbf{r})$ is formed according to* (14)*, using*

$$\hat{b}(r_n) = r_n \cdot \left\{ \sigma_W^2\sqrt{2/(\pi s)} \cdot \exp(\frac{-sr_n^2}{2\sigma_W^4}) + r_n \cdot \left[1 - \mathrm{erfc}(\sqrt{s/2} \cdot \frac{r_n}{\sigma_W^2})\right] \right\}^{-1} \tag{16}$$

where $s = \sigma_W^2\sigma_A^2/(\sigma_W^2 + \sigma_A^2)$.

This corollary follows from Theorem 3 in deriving the expression for $\hat{b}(r_n)$, which is straightforward. (However, it does not follow from Theorem 2, since the RAB channel is not a special case of the L-dimensional AWGN channel).

In the rest of the paper we will refer to the VQ decoder $\hat{\mathbf{X}}(\mathbf{r}) = \mathbf{T} \cdot \hat{\mathbf{h}}(\mathbf{r})$ as the *soft Hadamard column decoder* (SHCD), since the decoding is based on the soft Hadamard column (5). At this point we would like to identify some important advantages of the SHCD over the general form (3) of the MMSE decoder, assuming a binary channel for simplicity: (*i*) The SHCD is based on the *soft bit-estimates* (soft bits), $\hat{b}(r_n)$, which is conceptually appealing and of practical value since such estimates can be calculated from soft information already present in many practical systems; (*ii*) *Constrained versions* of the SHCD having lower decoding complexity are readily formulated. We will treat such decoders in Section 4 below; (*iii*) The concept of VQ by a *linear mapping of a block code* [29, 14], which has proven very useful for channel robust VQ-HD, is straightforwardly generalized to soft decoding using the SHCD as a basis. We will comment some more on this in Section 4; (*iv*) The Hadamard-based optimal decoder permits for an enlightening interpretation of how soft MMSE decoding is built up. The following sub-section is a discussion of this latter aspect.

3.2 Interpretation of the decoder structure

This sub-section provides an interpretation of the decoder structure. We assume a binary channel for simplicity, but we stress that the ideas are applicable to more general channels as well. In Figure 2 we have divided the decoding into three stages. The first stage, the *demodulation*, is the forming of $\hat{\mathbf{p}}(\mathbf{r})$ from the received vector $\mathbf{r}$, and named so since demodulation can be seen as an operation that converts the received data into a form more useful for decoding, and the subsequent stages operate on $\hat{\mathbf{p}}(\mathbf{r})$ to build the source vector estimate. The next stage, the forming of $\hat{\mathbf{h}}(\mathbf{r})$ from $\hat{\mathbf{p}}(\mathbf{r})$, is referred to as the *channel*

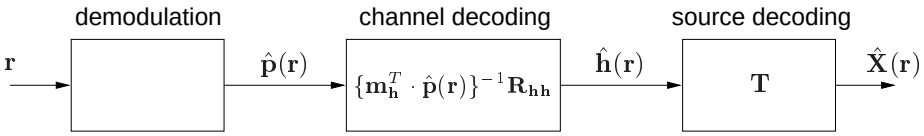

Figure 2: Separation of the decoding procedure.

decoding stage. To motivate this, consider that for full entropy encoding we have [c.f. the definition (9) of $\hat{\mathbf{p}}(\mathbf{r})$], that $\hat{\mathbf{h}}(\mathbf{r}) = \hat{\mathbf{p}}(\mathbf{r})$. On the other hand, if there is redundancy in the encoder output, then generally $\hat{\mathbf{h}}(\mathbf{r}) \neq \hat{\mathbf{p}}(\mathbf{r})$. Redundancy in the encoder output can be utilized by an MMSE decoder to counteract channel noise. Thus, the mapping from $\hat{\mathbf{p}}(\mathbf{r})$ to $\hat{\mathbf{h}}(\mathbf{r})$ can be interpreted as channel decoding in the sense that it makes use of the error protecting redundancy. Among the three decoding stages only the channel decoding uses the knowledge of the a-priori information $\{P_i\}$. The final stage in the decoding is the *source decoding*, where the estimate $\hat{\mathbf{h}}(\mathbf{r})$ of the Hadamard column $\mathbf{h}_I$ is mapped into the source space by the encoder matrix $\mathbf{T}$.

The separation of the decoding can be compared to the traditional approach for decoding, which is usually based on the ML-criterion (not taking information about the source statistics into account). This corresponds to the demodulation stage. The impact of a-priori knowledge can be *subsequently* accounted for by the channel decoding stage where the "ML-statistic" $\hat{\mathbf{p}}(\mathbf{r})$ is transformed into the "MMSE-statistic" $\hat{\mathbf{h}}(\mathbf{r})$.

3.3 Relation to the Hadamard transform and an algorithm for computations

Using the relationship between the Hadamard matrix and the Hadamard transform (Appendix A), it is straightforward to show that the components, $\{\mathbf{f}\}_n$, of the vector $\mathbf{f}(\mathbf{r}) = \mathbf{R}_{\mathbf{hh}}\hat{\mathbf{p}}(\mathbf{r})$ in (8), can be expressed in terms of the components, $\{\hat{\mathbf{p}}(\mathbf{r})\}_n$, of $\hat{\mathbf{p}}(\mathbf{r})$ as $\{\mathbf{f}\}_n = \sum_{m=0}^{N-1} \tilde{P}(n \oplus m)\{\hat{\mathbf{p}}(\mathbf{r})\}_m$ where $\{\tilde{P}(n)\}_{n=0}^{N-1}$ is the Hadamard transform of the encoder output probabilities $\{P_i\}_{i=0}^{N-1}$, and $\oplus$ denotes bit-wise modulo-2 addition. Furthermore, the scalar $\mathbf{m}_\mathbf{h}^T \cdot \hat{\mathbf{p}}(\mathbf{r})$ can be identified as $\{\mathbf{f}(\mathbf{r})\}_0$. Consequently, the nth component, $\hat{h}_n(\mathbf{r})$, of $\hat{\mathbf{h}}(\mathbf{r})$ can be expressed as

$$\hat{h}_n(\mathbf{r}) = \frac{\sum_{m=0}^{N-1} \tilde{P}(n \oplus m)\{\hat{\mathbf{p}}(\mathbf{r})\}_m}{\sum_{l=0}^{N-1} \tilde{P}(l)\{\hat{\mathbf{p}}(\mathbf{r})\}_l}. \tag{17}$$

Note that the numerator of (17) is a convolution of the sequences $\{\hat{\mathbf{p}}(\mathbf{r})\}_n$ and $\tilde{P}(n)$. Thus, since convolution corresponds to multiplication in the Hadamard-transform domain, (17) can easily be computed (see, e.g., [16]). Also, since the Hadamard transform is a fast transform, the complexity of the computation is of the order $N \cdot \log N$. For the special case of a binary channel, we provide a constructive proof of this claim in terms of an algorithm. The derivation of the algorithm is provided in Appendix C.

Algorithm for computing $\hat{\mathbf{h}}(\mathbf{r})$ in the case of a binary channel

Input data: The number of bits k, the probabilities $\{P_i\}_{i=0}^{N-1}$ and the bit-estimates $\{\hat{b}(r_l)\}_{l=1}^{k}$.

Output: The value of $\hat{\mathbf{h}}(\mathbf{r})$.

Let $\{\mathbf{f}_m^n\}_{n=0}^{N/2^m-1}$ be a sequence of column-vectors of size 2^m.

(0): *Initialization*; Set $\mathbf{f}_0^n = [P_n],\ n = 0, 1, \ldots, N-1$.

(1): *Recursive calculation of* $\mathbf{f}_k^0$ *from* $\mathbf{f}_0^0,\ \mathbf{f}_0^1, \ldots, \mathbf{f}_0^{N-1}$;

FOR $m = 1$ TO $m = k$

FOR $n = 0$ TO $n = N/2^m - 1$

$$\mathbf{f}_m^n = \begin{bmatrix} (1+\hat{b}(r_m))\mathbf{f}_{m-1}^{2n} + (1-\hat{b}(r_m))\mathbf{f}_{m-1}^{2n+1} \\ (1+\hat{b}(r_m))\mathbf{f}_{m-1}^{2n} - (1-\hat{b}(r_m))\mathbf{f}_{m-1}^{2n+1} \end{bmatrix} \tag{18}$$

END

END

(2): *Form* $\hat{\mathbf{h}}(\mathbf{r})$ *from* $\mathbf{f}_0^k$; Set $\hat{\mathbf{h}}(\mathbf{r}) = (\{\mathbf{f}_0^k\}_0)^{-1}\mathbf{f}_0^k$.

For a binary channel, the calculation of $\{\hat{b}(r_m)\}$ from $\mathbf{r}$ has a complexity proportional to the number of bits, k, (generally $k << N$), and the algorithm above requires an order of $N \log N$ operations to compute $\hat{\mathbf{h}}(\mathbf{r})$ from $\{\hat{b}(r_m)\}$. Remaining is a matrix multiplication to obtain $\hat{\mathbf{X}}(\mathbf{r})$. Hence, the overall complexity of decoding is, asymptotically, $N(C_1 \log N + C_2 d)$ where C_1 and C_2 are constants (not depending on N or d). Note that if the encoder matrix $\mathbf{T}$ is a sparse matrix (as in "LMBC-VQ", see Section 4 below), the decoding complexity can be significantly reduced since, in such a case, not all of the components of $\hat{\mathbf{h}}(\mathbf{r})$ are needed, and furthermore the complexity of the matrix multiplication $\mathbf{T}\hat{\mathbf{h}}(\mathbf{r})$ is reduced.

4 The Full Entropy Soft Hadamard Column Decoder

In this section, we investigate decoding for an encoder that gives

$$\Pr(I = i) = \frac{1}{N},\ \forall i. \tag{19}$$

We refer to such an encoder as a *full entropy encoder*, since $H(I) = k$. Note that we are implicitly assuming that the encoder is used on the source for which it was designed. That is, the encoder has full output entropy for this source, while it may have a lower entropy when used on other sources. Note also that the index probabilities of (19) can be used as maximum entropy estimates in the decoder design if the true index probabilities are unknown. This choice gives robustness to variations in the true probabilities.

Thus, the probabilities in (19) can either be the true ones or estimates, if the source is (partly) unknown[9]. We will refer to the encoder as a full entropy encoder in both cases.

Now we investigate the structure of the SHCD in the case of a full entropy encoder, assuming that the channel is a binary channel. Using (19) we have $\mathbf{R_{hh}} = N^{-1}\sum_{i=0}^{N-1}\mathbf{h}_i\mathbf{h}_i^T = \mathbf{I}$ and $\hat{\mathbf{p}}(\mathbf{r})^T\mathbf{m_h} = \hat{\mathbf{p}}(\mathbf{r})^T N^{-1}\sum_{i=0}^{N-1}\mathbf{h}_i = \hat{\mathbf{p}}(\mathbf{r})^T\cdot(1,0,\ldots,0)^T = 1$, giving the simple expression[10]

$$\hat{\mathbf{X}}(\mathbf{r}) = \mathbf{T}\cdot\hat{\mathbf{p}}(\mathbf{r}) \tag{20}$$

for the optimal decoder. Hence, MMSE decoding consists in this case of a linear mapping of the statistic $\hat{\mathbf{p}}(\mathbf{r})$. We name this form of the SHCD the *full entropy* SHCD (FE-SHCD). Note that the FE-SHCD is the optimal MMSE decoder for full encoder entropy over a binary channel. However, one may also regard the FE-SHCD as a sub-optimal, and less complex, alternative to the SHCD gaining close-to-optimal performance if the VQ has high, but less than full, encoder entropy. In such a case we will refer to the *structure* of the decoder as the FE-SHCD structure.

The encoder matrix, $\mathbf{T}$, is determined by the encoder centroids as $\mathbf{c}_i = \mathbf{T}\mathbf{h}_i,\ i = 0,1,\ldots,N-1$. To improve the performance when the entropy is not full, we can regard the matrix $\mathbf{T}$ as a free design parameter to be determined. That is, given the encoder and the FE-SHCD structure $\mathbf{T}\cdot\hat{\mathbf{p}}(\mathbf{r})$ on the decoder, determine the best matrix $\mathbf{T}$. To prevent confusion, we by $\mathbf{T}$ continue to denote the encoder matrix, and we let $\mathbf{A}$ be the parameter in the FE-SHCD structure. Using the MMSE-criterion we have $\mathbf{A}^* = \arg\min_{\mathbf{A}} E||\mathbf{X}-\mathbf{A}\cdot\hat{\mathbf{p}}(\mathbf{R})||^2$, (letting $\mathbf{A}^*$ denote the optimal value). Thus, $\mathbf{A}^*$ is given as

$$\mathbf{A}^* = \mathbf{R}_{\mathbf{x}\hat{\mathbf{p}}}(\mathbf{R}_{\hat{\mathbf{p}}\hat{\mathbf{p}}})^{-1} \tag{21}$$

where $\mathbf{R}_{\mathbf{x}\hat{\mathbf{p}}} = E[\mathbf{X}\hat{\mathbf{p}}(\mathbf{R})^T]$ and $\mathbf{R}_{\hat{\mathbf{p}}\hat{\mathbf{p}}} = E[\hat{\mathbf{p}}(\mathbf{R})\hat{\mathbf{p}}(\mathbf{R})^T]$. In the following we will refer to $\mathbf{A}^*\hat{\mathbf{p}}(\mathbf{r})$ as the *optimized* FE-SHCD (OFE-SHCD), since it is the optimal decoder chosen from the set of decoders that have the FE-SHCD structure.

An important feature of the FE-SHCD structure is that based on this still more constrained decoders can straightforwardly be constructed. To see this, note that the elements of $\mathbf{h}_i$ in the expansion $\mathbf{c}_i = \mathbf{T}\mathbf{h}_i$ for the encoder centroid $\mathbf{c}_i$ are formed according to (4) as bits and all possible products of different bits of the index i. In *VQ by a linear mapping of a block code* (LMBC-VQ), for VQ-HD [14], only the bits and a subset of the elements of $\mathbf{h}_i$ that are products of bits are used in the expansion for $\mathbf{c}_i$. A block channel code is utilized to describe which products (interpreted as "check bits" of the code) are to be used in the expansion. This technique is straightforwardly applicable also to VQ-SD using the FE-SHCD structure for decoding. The LMBC-VQ approach is in this case equivalent to using a mapping matrix $\mathbf{A}$

[9] Note that, besides the index probabilities, the encoder centroids have to be known in the decoder design. These also depend on the source, but are usually treated as a part of the VQ since they form the codebook of the VQ, and can often be assumed known even if the source is partly unknown.

[10] Note that this result also follows (perhaps more straightforwardly) from the *definition* of $\hat{\mathbf{p}}(\mathbf{r})$.

that has a (large) subset of its columns equal to zero. Thus the complexity of forming the product $\mathbf{A} \cdot \hat{\mathbf{p}}$ for decoding is significantly reduced. Also, the memory requirement is reduced, since a smaller matrix can be stored. The design techniques described in [14] can be used to design the encoder and the code that describes the structure of the mapping matrix $\mathbf{A}$. An application of LMBC-VQ with soft decoding to speech coding was presented in [27].

5 VQ Encoder and Decoder Design

This section considers the design of a VQ encoder/decoder *pair*. However, since the decoder is uniquely given when the source, the encoder and the channel are known, we consider the issue of encoder/decoder design as one of designing the *encoder*; when the encoder is known it specifies the optimal decoder. We consider the two approaches robust VQ with soft decoding (RVQ-SD) and channel optimized VQ with soft decoding (COVQ-SD), (as discussed in Section 1).

5.1 Encoder design for RVQ-SD

The problem of VQ-HD design is a well documented one [32]. For the RVQ approach an index assignment algorithm is required to give channel robustness. Several good such algorithms have been described (e.g., [8, 17, 18, 19]). In the RVQ-SD approach the Voronoi regions of a VQ-HD codebook, with a good index assignment, is applied to define the encoder. Thus, there is no complexity increase in the encoding, as compared to the hard decision equivalent, in utilizing the RVQ-SD approach.

5.2 Encoder design for COVQ-SD using the SHCD

A channel optimized VQ system is, as mentioned in Section 1, a system that is trained for a specific channel. In this case, the criterion for design includes the impact of the channel on the reproduction fidelity, and the design strives at finding an encoder (specifying a decoder) making the encoder/decoder pair jointly optimal for the given channel (according to the MMSE criterion).

One straightforward approach to system design is an alternating optimization approach, analogous to the generalized Lloyd algorithm [32]. That is, compute the optimal decoder for a fixed encoder, then compute the optimal encoder for this new decoder, and repeat. It is straightforward to derive an expression for the optimal (minimizing $D = D(\{\mathcal{S}_i\}) = E||\mathbf{X} - \delta(\mathbf{R})||^2$) encoder regions, $\{\mathcal{S}_i^*\}$, given an arbitrary but fixed decoder, $\delta(\mathbf{r})$, (c.f., [5, 7, 10, 9]). By writing the distortion, D, as

$$D = D(\{\mathcal{S}_i^*\}) = \sum_{i=0}^{N-1} \int_{\mathcal{S}_i^*} f_{\mathbf{X}}(\mathbf{x}) \left\{ \int f_{\mathbf{R}|I}(\mathbf{r}|i) ||\mathbf{x} - \delta(\mathbf{r})||^2 d\mathbf{r} \right\} d\mathbf{x} \tag{22}$$

we see, since $f_{\mathbf{X}}(\mathbf{x})$ is non-negative, that the vectors, $\mathbf{x}$, that shall be assigned to the ith optimal region, $\mathcal{S}_i^*$, are those that minimize the integral within brackets in (22). Consequently, we have, after some

manipulations, that

$$\mathcal{S}_i^* = \left\{ \mathbf{x} \in \mathbb{R}^d : \Sigma_i - \Sigma_j \leq 2\mathbf{x}^T(\mathbf{m}_i - \mathbf{m}_j),\ \forall j \right\} \tag{23}$$

where $\Sigma_i = E[||\delta(\mathbf{R})||^2 | I = i]$, and $\mathbf{m}_i = E[\delta(\mathbf{R}) | I = i]$. For the SHCD, $\delta(\mathbf{r}) = \hat{\mathbf{X}}(\mathbf{r}) = \mathbf{T}\hat{\mathbf{h}}(\mathbf{r})$, we have $\Sigma_i = \mathrm{tr}(\mathbf{T} \cdot E[\hat{\mathbf{h}}(\mathbf{R})\hat{\mathbf{h}}(\mathbf{R})^T | I = i] \cdot \mathbf{T}^T)$, and $\mathbf{m}_i = \mathbf{T} \cdot E[\hat{\mathbf{h}}(\mathbf{R}) | I = i]$. Using (23) it can be shown that the optimal encoder regions, $\mathcal{S}_i^*$, are convex polytopes. That is, convex regions that are bounded by hyperplanes. Consequently, an implication of (23) is that the encoder regions have the same kind of structure as Voronoi regions. As is well known the optimal encoder regions of a VQ-HD are Voronoi regions, or nearest neighbor regions. Thus, most of the various search algorithms applicable to VQ with hard decisions can be used for searching. This is an important feature for applications. Next, we formulate a design algorithm, based on (23), for a COVQ-SD system. (Entities calculated at the mth iteration are denoted by a subscript m.)

VQ encoder design for the SHCD (general channel)

(0) Let $\{\mathcal{S}_i\}_0$ be an initial partition. Set $m = 0$.

(1) Estimate $\{\mathbf{c}_i\}_m$ using the partition $\{\mathcal{S}_i\}_m$. Set $\mathbf{T}_m = N^{-1}\mathbf{C}_m\mathbf{H}$, where $\mathbf{C}_m$ is a matrix with the centroids $\{\mathbf{c}_i\}_m$ as columns. Also estimate $E[\hat{\mathbf{h}}(\mathbf{R})\hat{\mathbf{h}}(\mathbf{R})^T | I = i]_m$ and $E[\hat{\mathbf{h}}(\mathbf{R}) | I = i]_m$ for $i = 0, 1, \ldots, N-1$.

(2) Use $\Sigma_i = \mathrm{tr}(\mathbf{T}_m \cdot E[\hat{\mathbf{h}}(\mathbf{R})\hat{\mathbf{h}}(\mathbf{R})^T | I = i]_m \cdot \mathbf{T}_m^T)$ and $\mathbf{m}_i = \mathbf{T}_m \cdot E[\hat{\mathbf{h}}(\mathbf{R}) | I = i]_m$ in (23) to define a new partition $\{\mathcal{S}_i\}_{m+1}$. Set $m \leftarrow m + 1$.

(3) Repeat from (1) until convergence.

Using this algorithm we obtain a final partition $\{\mathcal{S}_i^*\}$ which, together with the source, defines the SHCD. In practice, expectations over the source are replaced by averages over a training set. The initial partition of step (0) can, e.g., be defined by the Voronoi regions of a RVQ-HD trained for the source under consideration. The convergence [step (3)] can be tested by any of the standard methods mentioned in [32], for example the relative improvement in performance can be used.

5.3 Encoder design for COVQ-SD using the FE-SHCD over a binary channel

We conclude this section with a discussion of the design of a VQ system employing the full-entropy SHCD (the FE-SHCD or the OFE-SHCD), assuming a binary channel. In this case, the only parameters depending on the channel statistics needed in the design are $E[\hat{\mathbf{p}}(\mathbf{R}) | I = i]$ and $E[\hat{\mathbf{p}}(\mathbf{R})\hat{\mathbf{p}}(\mathbf{R})^T | I = i]$. Letting $\mu = E[\hat{b}(R_n) | b_n(I) = +1]$, it can be shown that

$$\{E[\hat{\mathbf{p}}(\mathbf{R}) | I = i]\}_n = h_n(i) \cdot \mu^{w(n)} \tag{24}$$

and that

$$\{E[\hat{\mathbf{p}}(\mathbf{R})\hat{\mathbf{p}}(\mathbf{R})^T|I=i]\}_{n,m} = h_n(i)h_m(i)\cdot\mu^{w(n\oplus m)+w(n\circ m)} \tag{25}$$

where, $w(i)$ denotes the Hamming weight of the natural binary representation of the integer i, and the symbol "$\circ$" denotes the bit-wise AND operation. We state a design algorithm employing (24) and (25) to calculate the averages over the channel as follows:

VQ Encoder design for the FE-SHCD (binary channel)

Pre-calculate $\mu = E[\hat{b}(R_n)|b_n(I)=1]$, calculate and store $E[\hat{\mathbf{p}}(\mathbf{R})|I=i]$ and $E[\hat{\mathbf{p}}(\mathbf{R})\hat{\mathbf{p}}(\mathbf{R})^T|I=i]$ for $i=0,1,\ldots,N-1$, according to (24) and (25).

(0) Let $\{\mathcal{S}_i\}_0$ be an initial partition. Set $m=0$.

(1a) For the FE-SHCD, $\mathbf{T}\hat{\mathbf{p}}(\mathbf{r})$; Estimate $\{\mathbf{c}_i\}_m$ based on $\{\mathcal{S}_i\}_m$. Set $\mathbf{T}_m = N^{-1}\mathbf{C}_m\mathbf{H}$; *or*

(1b) For the OFE-SHCD, $\mathbf{A}\hat{\mathbf{p}}(\mathbf{r})$; Estimate $\{P_i\}_m$ and $\{\mathbf{c}_i\}_m$ based on $\{\mathcal{S}_i\}_m$. Use these in computing $\mathbf{R}_{\mathbf{x}\hat{\mathbf{p}}} = \sum_i P_i\mathbf{c}_i E[\hat{\mathbf{p}}(\mathbf{R})^T|I=i]$ and $\mathbf{R}_{\hat{\mathbf{p}}\hat{\mathbf{p}}} = \sum_i P_i E[\hat{\mathbf{p}}(\mathbf{R})\hat{\mathbf{p}}(\mathbf{R})^T|I=i]$ and set $\mathbf{A}_m = \mathbf{R}_{\mathbf{x}\hat{\mathbf{p}}}(\mathbf{R}_{\hat{\mathbf{p}}\hat{\mathbf{p}}})^{-1}$.

(2) Use $\Sigma_i = \mathrm{tr}(\mathbf{F}\cdot E[\hat{\mathbf{p}}(\mathbf{R})\hat{\mathbf{p}}(\mathbf{R})^T|I=i]\cdot\mathbf{F}^T)$ and $\mathbf{m}_i = \mathbf{F}\cdot E[\hat{\mathbf{p}}(\mathbf{R})|I=i]$ with $\mathbf{F}=\mathbf{T}_m$ or $\mathbf{F}=\mathbf{A}_m$ in (23) to define $\{\mathcal{S}_i\}_{m+1}$. Set $m\leftarrow m+1$.

(3) Repeat from (1) until convergence.

If the encoder entropy is full, the expression in step (1a) for $\mathbf{T}$ is the optimal one. Alternatively, if the FE-SHCD structure is used as an approximation to the optimal SHCD, using the OFE-SHCD as in step (1b) gives a better choice for the updating of the decoder. We emphasize that one major advantage of the FE-SHCD is that the entities $E[\hat{\mathbf{p}}(\mathbf{R})|I=i]$ and $E[\hat{\mathbf{p}}(\mathbf{R})\hat{\mathbf{p}}(\mathbf{R})^T|I=i]$ can be calculated and stored in *advance* of the training. This is a considerable saving compared to the general case where the corresponding parameters ($E[\hat{\mathbf{h}}(\mathbf{R})|I=i]$ and $E[\hat{\mathbf{h}}(\mathbf{R})\hat{\mathbf{h}}(\mathbf{R})^T|I=i]$) have to be estimated in *each* iteration.

6 On the Channel Distortion and the Structure of a Robust Encoder

In this section we discuss some aspects of channel robustness. We will concentrate the discussion to the encoder structure. The structure of the encoder, or more precisely of the *centroids* of the VQ encoder, is described by the encoder matrix $\mathbf{T}$.

6.1 On the channel distortion in the general case

First we consider the general case where the SHCD is used for decoding over a general channel and the encoder is arbitrarily chosen but known. The total distortion, D, can be split into two terms, the *quantization distortion* D_Q and the *channel distortion* D_C, according to (c.f., [17] for VQ-HD)[11]

$$D = E||\mathbf{X} - \hat{\mathbf{X}}(\mathbf{R})||^2 = E||\mathbf{X} - \mathbf{c}_I||^2 + E||\hat{\mathbf{X}}(\mathbf{R}) - \mathbf{c}_I||^2. \tag{26}$$

The quantization distortion, $D_Q = E||\mathbf{X} - \mathbf{c}_I||^2$, does not depend on the channel. Thus, in order to minimize the influence of the channel on the total distortion, D, the channel distortion, $D_C = E||\hat{\mathbf{X}}(\mathbf{R}) - \mathbf{c}_I||^2$, should be made as low as possible. Since $\hat{\mathbf{X}}(\mathbf{R})$ is the MMSE estimate of $\mathbf{c}_I$, we can (using the principle of orthogonality for MMSE estimation) rewrite the channel distortion as $D_C = E(\mathbf{c}_I^T[\mathbf{c}_I - \hat{\mathbf{X}}(\mathbf{R})])$. This expression can, in turn, be written as $D_C = \sum_i P_i D_C(i)$ where $D_C(i) \triangleq E(\mathbf{c}_I^T[\mathbf{c}_I - \hat{\mathbf{X}}(\mathbf{R})]|I = i)$. Defining $m_n(i) \triangleq E[\hat{h}_n(\mathbf{R})|I = i]$ and denoting by $\mathbf{t}_n$ the nth column of $\mathbf{T}$, we thus have

$$D_C(i) = E(\mathbf{c}_I^T[\mathbf{c}_I - \hat{\mathbf{X}}(\mathbf{R})]|I = i) = \sum_{m=0}^{N-1}\sum_{n=0}^{N-1} \mathbf{t}_m^T\mathbf{t}_n h_m(i)[h_n(i) - m_n(i)], \tag{27}$$

where $m_n(i)$ can be expressed as

$$m_n(i) = E\left[\frac{\sum_{l=0}^{N-1}\tilde{P}(l\oplus n)\{\hat{\mathbf{p}}(\mathbf{R})\}_l}{\sum_{j=0}^{N-1}\tilde{P}(j)\{\hat{\mathbf{p}}(\mathbf{R})\}_j}|I = i\right]. \tag{28}$$

In (28) we have used the Hadamard transform expression (17) for $\hat{h}_n$. We can see that the channel distortion is dependent on the channel through the value of $m_n(i)$ only and, as intuition suggests, $D_C(i)$ is low if $m_n(i)$ is close to $h_n(i)$. Unfortunately, a tractable expression for $m_n(i)$ is hard to find in the general case, where the encoder indices have redundancy and the SHCD is used over a general channel. Because of this, we restrict the rest of this section to some special cases which can be handled in some more detail.

Examining expression (27) further, we note that for encoder/decoder pairs and channels giving $m_n(i)$ the form $m_n(i) = h_n(i)\cdot\nu_n$, where ν_n is a positive number independent of the index i, we get $D_C(i) = \sum_{m=0}^{N-1}\sum_{n=0}^{N-1}\mathbf{t}_m^T\mathbf{t}_n \cdot h_m(i)h_n(i)[1-\nu_n]$. As we shall see, one example where $m_n(i) = h_n(i)\cdot\nu_n$ holds, is full entropy encoding over a binary channel. Now, taking expected value with respect to the encoder indices we have

$$D_C = \sum_{m=0}^{N-1}\sum_{n=0}^{N-1}\mathbf{t}_m^T\mathbf{t}_n\tilde{P}(m\oplus n)(1-\nu_n), \tag{29}$$

[11] Note that this division into D_Q and D_C is *always* valid since it is made with respect to the "reference vectors" $\{\mathbf{c}_i\}$, where $\mathbf{c}_i = E[\mathbf{X}|I = i]$ are the encoder centroids. If the split is not made with respect to the centroids, then generally a mixed-term distortion has to be included (c.f. [17] and Sections 3.5–6 of [16]).

where (as before) $\{\tilde{P}(n)\}_{n=0}^{N-1}$ is the Hadamard transform of $\{P_i\}_{i=0}^{N-1}$. Moreover, with the additional assumption of full encoder entropy it is straightforward to show that $\tilde{P}(n) = 0,\ n > 0$, giving

$$D_c = \sum_{n=0}^{N-1} ||\mathbf{t}_n||^2(1 - \nu_n). \tag{30}$$

The next sub-section considers the implications of (30) in the special case of a binary channel with full entropy encoding.

6.2 Full entropy encoder and a binary channel

Assuming full encoder entropy we have $\hat{\mathbf{h}}(\mathbf{r}) = \hat{\mathbf{p}}(\mathbf{r})$, and for a binary channel we get, employing (24), that $m_n(i) = h_n(i)\mu^{w(n)}$. Note that $\mu \geq 0$, thus $h_n(i)$ enters as the sign of $m_n(i)$. Consequently $m_n(i)$ is of the form $m_n(i) = h_n(i)\nu_n$, with $\nu_n = \mu^{w(n)}$. Employing $\nu_n = \mu^{w(n)}$ in (30), we have

$$D_c = \sum_{n=1}^{N-1} ||\mathbf{t}_n||^2(1 - \mu^{w(n)}). \tag{31}$$

A similar expression (cited in (33) below) valid for VQ-HD over a binary symmetric channel was presented in [12] (see also [14, 33, 19]). To proceed further, we consider the class of encoders where members have the same value of the quantity $P_T \triangleq \sum_{n=1}^{N-1} ||\mathbf{t}_n||^2$. This is, for example, the case when the (unordered) set of centroids $\{\mathbf{c}_i\}$ is common among the encoders of the class. We name such a set of encoders a class of P_T-*constrained encoders*, using the value of P_T to denote the class. Now, observing that $0 \leq \mu < 1$, we have the important result that

$$D_C = \sum_{n=1}^{N-1} (1 - \mu^{w(n)})||\mathbf{t}_n||^2 \geq (1 - \mu) \sum_{n=1}^{N-1} ||\mathbf{t}_n||^2 = (1 - \mu)P_T \tag{32}$$

with equality iff $w(n) > 1 \Rightarrow \mathbf{t}_n = \mathbf{0}$. Thus, using (32), we have a characterization of the best (in terms of minimal channel distortion) possible encoder, within the class of a fixed P_T . If there exists an encoder/decoder pair for which $w(n) > 1 \Rightarrow \mathbf{t}_n = \mathbf{0}$ holds, then this is the best possible pair[12]. To examine further what this condition means, consider the expansion $\mathbf{c}_i = \sum_{n=0}^{N-1} \mathbf{t}_n h_n(i)$. If $w(n) > 1 \Rightarrow \mathbf{t}_n = \mathbf{0}$, then $\mathbf{c}_i = \mathbf{t}_0 + \sum_{n=1}^{k} \mathbf{t}_{2^{n-1}} b_n(i)$. We see that this means that the encoder has to have such structure that the ith centroid $\mathbf{c}_i$ can be described by a linear combination of k of the vectors, $\mathbf{t}_n$, with the bits of the index i as weights. Hence, no products of bits are allowed to enter the Hadamard expansion for $\mathbf{c}_i$. Consequently, this kind of structure can be described as a linear mapping from the hypercube $\{\pm 1\}^k$ to $\mathbb{R}^d$. We say that a VQ encoder possessing such structure is *linear*. This linearity result is a generalization of the corresponding result for full entropy VQ-HD given in [19, 33]. Note that (31) can be utilized to determine the quality of the IA of a RVQ-SD system. This follows since all encoders resulting from

[12] We refer to the encoder/decoder *pair* as optimal (minimum channel distortion), since it may be the case that the encoder/decoder is obtained through a procedure that optimizes the pair. In this sense the resulting encoder, defining the encoder matrix, depends on the corresponding decoder.

different IAs on a fixed set of centroids belong to the same P_T-constrained class. The best mapping from $\mathbf{b}_i$ to $\mathbf{c}_i$ is linear. However, for an arbitrary full entropy encoder there may be no linear description of the centroids. Then the number $(1-\mu)P_T$ serves as a useful lower bound to the channel distortion over all IAs.

The expression for the channel distortion in a full entropy system can also be utilized in comparing hard and soft decoding. To make such a comparison we cite, from [19], the expression

$$D_C^{\text{hard}} = 2\sum_{n=1}^{N-1} ||\mathbf{t}_n||^2(1-(1-2q)^{w(n)}) \tag{33}$$

for the channel distortion of full entropy VQ-HD over a binary symmetric channel of crossover probability q. It is easily shown that $D_C^{\text{hard}} \geq 4qP_T$, [(33) was utilized in [19] to prove that the lower bound $4qP_T$ to D_C^{hard} is met by a linear encoder mapping]. Now, to proceed, assume that we have a fixed encoder characterized by its centroids. Assume, moreover, that the Voronoi regions of the centroids are used as encoder regions, and that the resulting encoder is a full entropy encoder. Then we can form the ratio

$$\theta \triangleq \frac{D_C^{\text{soft}}}{D_C^{\text{hard}}} = \frac{\sum_{n=1}^{N-1} ||\mathbf{t}_n||^2(1-\mu^{w(n)})}{2\sum_{m=1}^{N-1} ||\mathbf{t}_m||^2(1-(1-2q)^{w(m)})} \tag{34}$$

between the resulting channel distortion of the optimal soft decoding system and an ordinary VQ-HD decoder, employing the centroids as codebook vectors. Assume, furthermore, that the centroids have such structure that the encoder can be made linear, then we have the ratio between the minimum possible channel distortions as

$$\theta_{\text{opt}} \triangleq \frac{(1-\mu)P_T}{4qP_T} = \frac{(1-\mu)}{4q}. \tag{35}$$

The ratio θ_{opt} is depicted in Figure 3, for the KAB channel versus the corresponding hard channel.

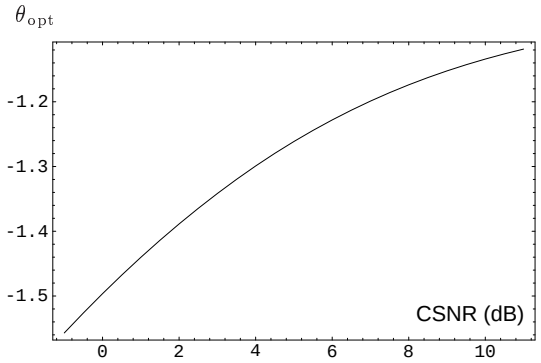

Figure 3: The ratio θ_{opt} (in dB) as a function of the CSNR.

In Figure 3 we can observe that the gain of soft decoding, in terms of lower channel distortion, varies between 1 and 1.6 dB in the CSNR interval under consideration. One fact that contributes to the gain is

that the soft decoder as allowed to adapt to a varying CSNR. We comment that the gain of VQ-SD over VQ-HD is generally larger for encoders not having optimal IAs (see Section 7.2 for a discussion). Hence, in practice the gain is often larger than what is suggested by Figure 3.

6.3 Binary channel without the full entropy assumption: Spherically invariant codes

If the encoder entropy is not full, the FE-SHCD is generally sub-optimal, and we have to include more terms in the expression for the channel distortion. Again assuming a binary channel, it can be shown that

$$D_C(i) = \sum_{n=1}^{N-1} \sum_{m=1}^{N-1} \mathbf{t}_n^T \mathbf{t}_m h_n(i) h_m(i) f_{n,m}, \tag{36}$$

where $f_{n,m} \triangleq 1 - \mu^{w(n)} - \mu^{w(m)} + \mu^{w(n \circ m) + w(n \oplus m)}$. Note that $f_{n,m}$ is non-negative[13]. The expression (36) is considerably more difficult to handle than the full entropy expression (31). Therefore, we treat only a specially restricted class of encoders for which the channel distortion expression becomes tractable. As we will see, such an analysis can give some insight in how the channel robustness is affected when the transmitted indices contain redundancy. Hence, consider the class consisting of encoders fulfilling $\sum_{n \neq m} \mathbf{t}_n^T \mathbf{t}_m h_n(i) h_m(i) f_{n,m} = f_{r,s} \sum_{n \neq m} \mathbf{t}_n^T \mathbf{t}_m h_n(i) h_m(i)$ for some pair of integers $0 < r, s \leq N-1$. For such a class we have

$$\begin{aligned} D_C(i) &= \sum_{n=1}^{N-1} ||\mathbf{t}_n||^2 (1 - \mu^{w(n)}) + \sum_{n \neq m} \mathbf{t}_n^T \mathbf{t}_m h_n(i) h_m(i) f_{n,m} \\ &= \sum_{n=1}^{N-1} ||\mathbf{t}_n||^2 (1 - \mu^{w(n)}) + f_{r,s} \sum_{n \neq m} \mathbf{t}_n^T \mathbf{t}_m h_n(i) h_m(i) \\ &= \sum_{n=1}^{N-1} ||\mathbf{t}_n||^2 (1 - \mu^{w(n)}) + f_{r,s} (||\mathbf{c}_i - \mathbf{t}_0||^2 - P_T). \end{aligned} \tag{37}$$

Consequently, in this case the channel distortion (given a transmitted index, i) is dependent on the index, i, through the term $||\mathbf{c}_i - \mathbf{t}_0||^2$ only. Note that $\mathbf{t}_0 = N^{-1} \sum_n \mathbf{c}_n$, that is, $\mathbf{t}_0$ is the algebraic mean of the centroids. Thus $||\mathbf{c}_i - \mathbf{t}_0||^2$ is the squared distance from the ith centroid to the average of the centroid set. Since all centroid vectors at the same distance from $\mathbf{t}_0$ have the same channel distortion behavior for the class of encoders which satisfy $\sum_{n \neq m} \mathbf{t}_n^T \mathbf{t}_m h_n(i) h_m(i) f_{n,m} = f_{r,s} \sum_{n \neq m} \mathbf{t}_n^T \mathbf{t}_m h_n(i) h_m(i)$, this class is named the class of *spherically invariant* codes with parameters r and s (see also [15] pp. 330-331)[14].

[13] $f_{n,m} = (1 - \mu^{w(n)})(1 - \mu^{w(m)}) + \mu^{w(n \circ m) + w(n \oplus m)} - \mu^{w(n)+w(m)} \geq \mu^{w(n \circ m) + w(n \oplus m)} - \mu^{w(n)+w(m)} \geq \mu^{2w(n \circ m) + w(n \oplus m)} - \mu^{w(n)+w(m)} = 0$, since $0 \leq \mu < 1$ and $w(n) + w(m) = 2w(n \circ m) + w(n \oplus m)$.

[14] The term "spherically invariant" refers to the fact that $D_C(i)$ does not depend on the *direction* from $\mathbf{t}_0$ to $\mathbf{c}_i$ but only on the *distance* $||\mathbf{c}_i - \mathbf{t}_0||$. Hence, all centroids on a sphere centered at $\mathbf{t}_0$ give the same contribution to $D_C(i)$, and in this sense the code is spherically invariant with respect to channel distortion.

Now, in averaging over the encoder indices in (37), we have

$$D_C = \sum_{n=1}^{N-1} ||\mathbf{t}_n||^2(1-\mu^{w(n)}) + f_{r,s}(V_C - P_T) \tag{38}$$

where we have defined $V_C = E||\mathbf{c}_I - \mathbf{t}_0||^2$. We see that the first term, $\sum_{n=1}^{N-1} ||\mathbf{t}_n||^2(1-\mu^{w(n)})$, of this expression is the channel distortion for a full entropy system having the same encoder matrix [c.f. Eq. (31)]. Furthermore, for source pdfs which decrease exponentially with the distance from the mean, such as the Gaussian or the Laplacian pdfs, we generally have that $V_C < P_T$. Hence, since $f_{r,s}$ is non-negative, $f_{r,s}(V_C - P_T)$ is negative (or zero). This illustrates that a spherically invariant code can give a lower channel distortion, than can a full entropy encoder having the same encoder matrix. Thus, using one particular example we have illustrated that redundancy in the encoder output can be used to lower the channel distortion as compared to the full entropy case.

7 Numerical Results

In this section we present numerical results and comparisons. First we present results for RVQ-SD versus RVQ-HD. We have simulated the SHCD, the FE-SHCD and the OFE-SHCD. Then we investigate the ability of soft decoding to counteract large errors and bad IAs. The section is concluded with results for COVQ-HD versus COVQ-SD.

In all simulations we have assumed a binary channel (the KAB or the RAB channel). In the VQ-HD results the output of the corresponding hard channel (defined in Section 2.2) has been used in a table look-up. In the RVQ-HD results the encoder centroids have been used as codevectors, and in the COVQ-HD results the optimal codevectors [7] have been used. In the simulations we consider first order Gauss-Markov sources with correlation a, modeled as $X_n = aX_{n-1} + U_n$ where $\{U_n\}$ is iid Gaussian. The vectors of the corresponding vector source (c.f., Section 2.1) are obtained as $\mathbf{X}_t = [X_{td}, \ldots, X_{(t-1)d+1}]^T$. The source obtained for $a = 0$ is the iid Gaussian source. Performance is in most cases measured in terms of the output SNR, $E||\mathbf{X}||^2/E||\mathbf{X} - \hat{\mathbf{X}}||^2$ (abbreviated as "SNR" below).

A good index assignment is required in RVQ-SD. We have used the linearity increasing swap algorithm (LISA) of [19] and the simulated annealing approach of [7]. The LISA makes the encoder of an RVQ-HD maximally linear. From the discussion in Section 6 we know that such IAs are good also for RVQ-SD, if the encoder has high entropy. In some cases, when the encoder has much redundancy, we have utilized the simulated annealing approach instead. In lacking theoretical tools in cases when the entropy is not full, we have observed that an algorithm giving a good IA for RVQ-HD also gives a good IA for RVQ-SD.

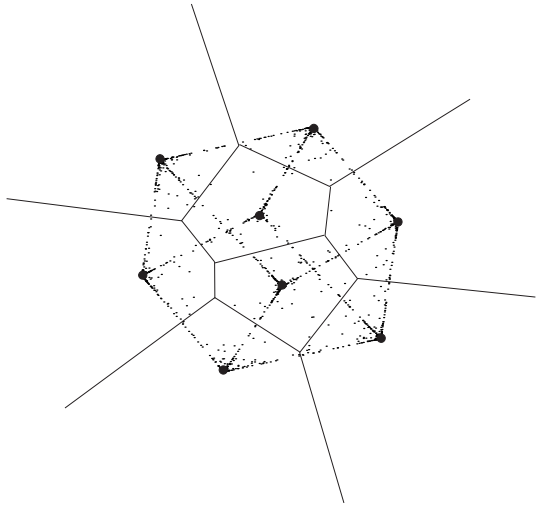

Figure 4: Source vector estimates, $\hat{\mathbf{X}}$, produced by the SHCD. The encoder is defined by an RVQ with k=3 bits and d=2 dimensions. The source is iid Gaussian. Estimates can be observed as small dots. The larger dots mark the locations of the encoder centroids and the solid lines mark the boundaries of the encoder regions.

7.1 Illustrating soft decoding

Figure 4 illustrates the principle of soft decoding. In this simulation the encoder is defined by the Voronoi regions of a RVQ-HD, trained for an iid Gaussian source. Source vector estimates, as obtained when using the SHCD on the KAB channel, are marked by small dots. We can see estimates marking out lines between centroids having indices that differ in one bit only. When there is an "uncertainty" about which index was sent, the decoder compensates this by moving the estimate towards the second most probable vector. Thus, instead of choosing a codevector (that might be the wrong one), the soft decoder outputs an average over the most probable codevectors [c.f., Eq. (3)]. In many applications this averaging not only lowers the mean-square error, but also gives errors a more "pleasant" appearance. In image coding, for example, hard decoding tends to give errors that are very distinct and easy to observe while soft decoding gives errors a "smoother" appearance [25].

7.2 Comparing hard and soft decoding for a fixed encoder

A comparison between hard and optimal soft decoding is depicted in Figure 5. The channel is the KAB channel, the source is a first order Gauss-Markov source with correlation 0.9, and the encoder is fixed and defined by the Voronoi regions of an RVQ-HD trained for the source. As we can see, soft decoding clearly performs better than hard decoding. At an output SNR of 4 dB, for example, the gain is approximately 2 dB in CSNR. Noteworthy is also the small difference between the optimal SHCD and the FE-SHCD in this simulation. This latter fact is due to the high encoder entropy (5.87 bits compared to the full entropy of 6 bits). In Figure 6 we compare the SHCD, the OFE-SHCD and the FE-SHCD for an encoder with low encoder entropy (4.76 bits compared to the full entropy of 6 bits). (This encoder was obtained from training a COVQ-HD over a channel with a BER of 5%.) As we can see the difference between the

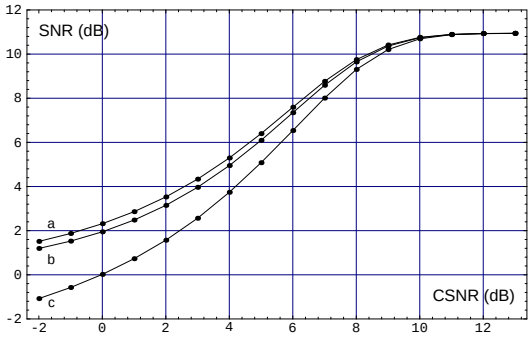

Figure 5: Comparison in terms of SNR vs. CSNR between the SHCD, the FE-SHCD and hard decoding. The source is first order Gauss-Markov with correlation 0.9. The dimension is $d = 6$ and the rate is $R = 1$ bit per dimension. (a) The SHCD; (b) The FE-SHCD; (c) Hard decoding. The same encoder is used in all cases. The encoder entropy is 5.87 bits.

SHCD and the FE-SHCD is more prominent in this simulation. Note, however, that the performance of the OFE-SHCD is close to that of the SHCD. One conclusion that can be drawn from this example is thus that the OFE-SHCD can give performance close to that of the SHCD, despite its suboptimal structure, also for encoders not having high entropy.

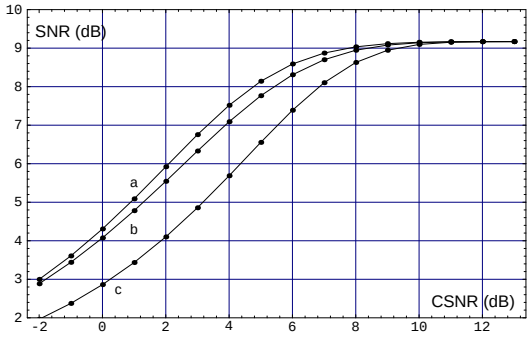

Figure 6: Comparison between the SHCD and the FE-SHCD. First order Gauss-Markov source with correlation 0.9. The dimension is $d = 6$ and the rate $R = 1$ bit per dimension. (a) The SHCD; (b) The OFE-SHCD; (c) The FE-SHCD. The same encoder is used in all cases. The encoder entropy is 4.76 bits.

For some applications the number of large errors is as least as important a measure of performance as is the mean-square error. Figure 7 illustrates the ability of the SHCD to counteract large errors. This figure shows the relative number of estimates giving a squared error $||\mathbf{X} - \hat{\mathbf{X}}||^2$ larger than $0.5E||\mathbf{X}||^2$. As we can see the SHCD gives fewer such large errors than the hard decoder and the gain increases for bad channels. Hence, soft decoding can give advantages in applications, such as image coding (c.f., [25]) and in coding the spectral information of a speech coder (c.f., [27]), where large errors can be very annoying. A related comparison is made in Figure 8, where the performance is investigated for two different IAs (a good and a bad). We can see that the SHCD counteracts a bad IA in the sense that the difference in performance between the two IAs is more prominent when using hard decoding. Thus, the relative gain of soft over hard decoding is higher for encoders with a bad IA. This is also a useful feature in applications, since finding a good IA is generally very difficult for large codebooks. Soft decoding can be applied to counteract the imperfections of a suboptimal IA.

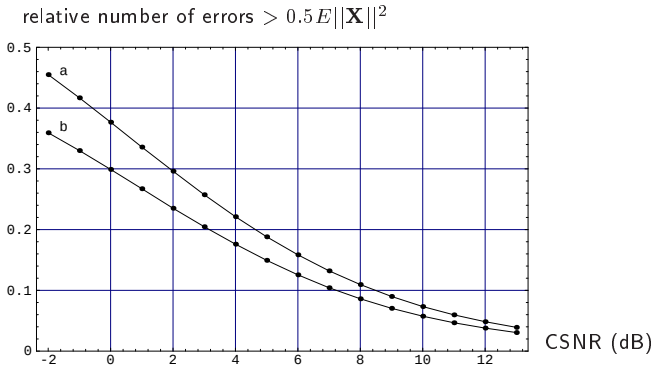

Figure 7: The relative number of source vector estimates $\hat{\mathbf{X}}$ giving an error $||\mathbf{X} - \hat{\mathbf{X}}||^2$ greater than $0.5E||\mathbf{X}||^2$. Gauss-Markov source with correlation 0.9. The KAB channel. The encoder is defined by an RVQ in both cases, $k = 6$ bits and $d = 6$ dimensions. (a) Hard decoding; (b) The SHCD.

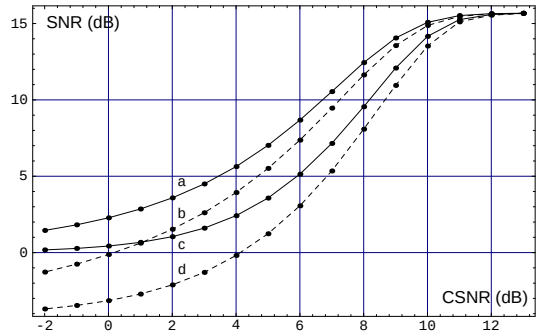

Figure 8: The difference between a bad IA and a good IA. A Gauss-Markov source with correlation 0.9, encoder with $d = 4$ and $k = 8$ trained for a noiseless channel. Encoder entropy 7.85 bits. (a): Good IA and the SHCD; (b): Good IA and hard decoding; (c): Bad (random) IA and the SHCD; (d): Bad IA and hard decoding. The channel is the KAB channel in all cases.

7.3 Channel optimized VQ

Figure 9 illustrates the encoder regions for two different 4-bit 2-dimensional encoders. To the left are the encoder regions of an encoder trained for a noiseless channel, and to the right we see the encoder regions of an encoder trained for the SHCD over a KAB channel with a CSNR of 2.15 dB (corresponding to a BER of 10%). Note that 3 regions are empty in the latter case. In the experiments, we have observed that generally more encoder regions become empty sets when the encoder is trained for a soft decoder than when the encoder is trained for hard decoding over the corresponding hard channel. Hence, the encoder provides a higher amount of redundancy when trained for soft decoding.

For reference purposes, Tables 1 and 2 list the dth order OPTA functions at the specific CSNRs that were used in the COVQ design. The dth order OPTA (optimal performance theoretically achievable) function $\Delta_d(R)$ can be computed as $\Delta_d(R) = D_d(R \cdot C)$ where D_d is the dth order distortion-rate function of the source [34], R is the rate of the VQ in bits per dimension and C is the capacity, in bits per channel use, of the binary channel. It serves as a lower bound to the performance of rate-R and dimension-d VQ systems over the given channel, and gives an achievable lower bound as the dimension goes to infinity, $d \to \infty$. In the tables the OPTA is expressed in terms of SNR, that is, $E||\mathbf{X}||^2/\Delta_d(R)$.

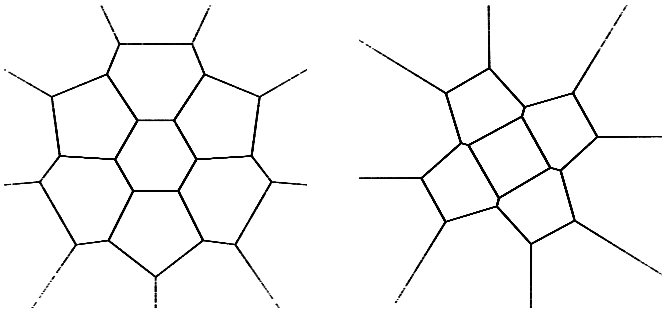

Figure 9: Encoder regions for encoders trained for an iid Gaussian source. The dimension is $d = 2$ and the rate is $R = 2$ bits per dimension. **Left**: An encoder trained for a noiseless channel; **Right**: An encoder trained for the KAB channel with a CSNR corresponding to a BER of 10%.

Table 1: The OPTA function of order d for rate $R = 1$ VQs over the KAB channel. First order Gauss-Markov sources of correlations 0 and 0.9. The OPTA is given in terms of SNR (in dB)

	correlation 0.0			correlation 0.9			
BER	$d = 4$	$d = 6$	$d = 8$	$d = 4$	$d = 6$	$d = 8$	CSNR [dB]
0.001	5.996	5.996	5.996	11.38	12.00	12.30	9.799
0.005	5.899	5.899	5.899	11.28	11.90	12.21	8.218
0.010	5.783	5.783	5.783	11.16	11.78	12.09	7.333
0.050	4.915	4.915	4.915	10.21	10.85	11.18	4.322
0.100	3.940	3.940	3.940	8.994	9.693	10.04	2.154

Tables 3 through 5 contain results for COVQ-HD and COVQ-SD. For COVQ-SD both the SHCD and the OFE-SHCD have been investigated. The results were obtained as follows: (*i*) The channel (the CSNR) was fixed, and the training was initialized using an RVQ-HD system; (*ii*) A COVQ-HD was trained (c.f., [7]) for the corresponding hard binary channel; (*iii*) Using this COVQ-HD as initialization the COVQ-SD was trained employing the results of Section 5. Tables 3 and 4 show the performance of COVQ-SD and COVQ-HD over the KAB channel for an iid Gaussian source and a first order Gauss-Markov source of correlation 0.9, respectively. We can observe that the performance of COVQ-SD is better in all cases. Note also that the difference between hard and soft decoding becomes larger as the channel noise grows. For the OFE-SHCD we note that the performance coincides with that of the SHCD when the encoder entropy is full. This is the case in Table 3, for the iid source. Here, all encoders have (almost) full entropies. On the other hand, when there is redundancy in the encoder output, as is the case in Table 4, the SHCD performs better than the OFE-SHCD. Note, however, that the OFE-SHCD still performs significantly better than COVQ-HD. In Table 5 we have listed the results when the systems were designed for the RAB channel and a first order Gauss-Markov source of correlation 0.9. The performance follows the same trends as for the KAB channel.

The evaluation of the COVQ systems were made at the same CSNRs as those for which the systems were trained. We have observed, though, that the performance is not critically sensitive for mismatch of the encoder with respect to the channel. Regarding the match of the decoder to the channel it is more reasonable in practice to assume perfect knowledge of the channel at the receiver than at the transmitter.

Table 2: The OPTA function of order d for rate $R = 1$ VQs over the RAB channel. First order Gauss-Markov sources of correlations 0 and 0.9. The OPTA is given in terms of optimum SNR (in dB)

	correlation 0.0			correlation 0.9			
BER	$d = 4$	$d = 6$	$d = 8$	$d = 4$	$d = 6$	$d = 8$	CSNR [dB]
0.001	5.998	5.998	5.998	11.39	12.00	12.31	26.98
0.005	5.910	5.910	5.910	11.29	11.91	12.22	19.93
0.010	5.801	5.801	5.801	11.18	11.80	12.11	16.86
0.050	4.959	4.959	4.959	10.26	10.90	11.22	9.308
0.100	3.984	3.984	3.984	9.053	9.749	10.09	5.509

Also, the soft decoder is more straightforwardly updated according to a varying channel than is the encoder.

Table 3: SNR in dB for various rate $R = 1$ (bits per dim) systems trained for the KAB channel with soft decoding and hard decoding. The SHCD and the OFE-SHCD have been employed for decoding in the COVQ-SD results. The source is in all cases the iid Gaussian source.

	BER	0.001	0.005	0.01	0.05	0.10
	CSNR [dB]	9.799	8.218	7.333	4.322	2.154
SHCD	$d = 8$	4.86	4.64	4.46	3.42	2.61
	$d = 6$	4.72	4.57	4.40	3.41	2.60
	$d = 4$	4.58	4.45	4.30	3.40	2.61
OFE-SHCD	$d = 8$	4.86	4.64	4.46	3.42	2.61
	$d = 6$	4.72	4.57	4.40	3.41	2.60
	$d = 4$	4.58	4.45	4.30	3.40	2.61
HARD	$d = 8$	4.83	4.56	4.32	3.13	2.27
	$d = 6$	4.68	4.50	4.30	3.15	2.26
	$d = 4$	4.56	4.39	4.21	3.15	2.27

8 Summary and Conclusions

We have addressed the problem of transmitting a source via vector quantization over a channel producing an analog (unquantized) output. The decoder of the system utilizes the analog channel output for estimation of the transmitted vector. Such decoding is referred to as soft decoding. We have introduced a decoder, the soft Hadamard column decoder (SHCD), being optimal in the sense of minimum mean-square error, and we have investigated some special cases of the optimal decoder having certain structure and lower complexity. We have also presented an algorithm for decoding and provided an interpretation of how the decoding is built up in terms of demodulation, channel decoding and source decoding. Furthermore, we have treated the system design problem, both for the optimal decoder and the suboptimal versions. Moreover, we have analyzed the distortion introduced by the channel and provided results regarding the structure of a robust system. Finally, we have investigated the performance of the proposed systems in terms of numerical simulations.

The simulations confirmed that the SHCD gives better performance than the corresponding hard decoders. The simulations also demonstrated that the constrained versions of the SHCD can give good

Table 4: SNR in dB for various rate $R = 1$ (bits per dim) systems trained for the KAB channel with soft decoding and hard decoding. The SHCD and the OFE-SHCD have been employed for decoding in the COVQ-SD results. The source is in all cases the first-order Gauss-Markov source with correlation 0.9.

	BER	0.001	0.005	0.01	0.05	0.10
	CSNR [dB]	9.799	8.218	7.333	4.322	2.154
SHCD	$d = 8$	11.2	10.6	10.2	8.48	6.89
	$d = 6$	10.8	10.1	9.63	7.84	6.21
	$d = 4$	10.0	9.40	8.77	7.04	5.69
OFE-SHCD	$d = 8$	11.2	10.5	10.1	8.03	6.43
	$d = 6$	10.8	10.1	9.54	7.34	5.78
	$d = 4$	10.0	9.36	8.73	6.68	5.29
HARD	$d = 8$	11.1	10.3	9.80	7.51	5.81
	$d = 6$	10.7	9.94	9.23	6.83	5.16
	$d = 4$	9.92	9.13	8.38	6.24	4.67

Table 5: SNR in dB for various rate $R = 1$ (bits per dim) systems trained for the RAB channel with soft decoding and hard decoding. The SHCD and the OFE-SHCD have been employed for decoding in the COVQ-SD results. The source is in all cases the first-order Gauss-Markov source with correlation 0.9.

	BER	0.001	0.005	0.01	0.05	0.10
	CSNR [dB]	26.98	19.93	16.86	9.308	5.509
SHCD	$d = 8$	11.2	10.6	10.3	8.54	6.95
	$d = 6$	10.8	10.2	9.67	7.94	6.27
	$d = 4$	10.1	9.46	8.86	7.11	5.45
OFE-SHCD	$d = 8$	11.2	10.5	10.1	8.06	6.46
	$d = 6$	10.8	10.2	9.57	7.38	5.80
	$d = 4$	10.0	9.38	8.75	6.74	5.33
HARD	$d = 8$	11.1	10.2	9.79	7.51	5.81
	$d = 6$	10.7	9.92	9.22	6.81	5.15
	$d = 4$	9.94	9.12	8.37	6.26	4.69

performance at lower complexity. Moreover, the soft decoder counteracts large errors and bad index assignments, which is a valuable feature in many applications.

Appendix A: Hadamard Matrices for VQ Description

A (Sylvester-type) Hadamard matrix, $\mathbf{H}_k$, of size $N = 2^k$ is a symmetric square matrix with elements from $\{\pm 1\}$, which is defined recursively as

$$\mathbf{H}_1 = \begin{bmatrix} +1 & +1 \\ +1 & -1 \end{bmatrix}; \quad \mathbf{H}_k = \mathbf{H}_1 \otimes \mathbf{H}_{k-1},\ k > 1,$$

where the symbol $\otimes$ denotes the Kronecker product, i.e., for two matrices $\mathbf{A}$ and $\mathbf{B}$ we have

$$\mathbf{A} \otimes \mathbf{B} = \begin{bmatrix} \{\mathbf{A}\}_{0,0}\mathbf{B} & \cdots & \{\mathbf{A}\}_{0,m-1}\mathbf{B} \\ \vdots & \ddots & \vdots \\ \{\mathbf{A}\}_{n-1,0}\mathbf{B} & \cdots & \{\mathbf{A}\}_{n-1,m-1}\mathbf{B} \end{bmatrix}$$

if $\mathbf{A}$ is of size n rows and m columns. The recursive nature of the Hadamard matrix gives the useful feature that when letting the natural binary representation of the integer i be $(b_k, b_{k-1}, \ldots, b_1)$, with logical "zero" represented by $+1$ and logical "one" by -1, we have that

$$\mathbf{h}_i = \begin{bmatrix} 1 \\ b_k \end{bmatrix} \otimes \begin{bmatrix} 1 \\ b_{k-1} \end{bmatrix} \otimes \cdots \otimes \begin{bmatrix} 1 \\ b_1 \end{bmatrix}$$

where $\mathbf{h}_i$ denotes the ith column of $\mathbf{H}_k$. Another useful property of the Hadamard matrix is that, for any size $N = 2^k$, we have $\mathbf{H}_k \cdot \mathbf{H}_k = N \cdot \mathbf{I}$, where $\mathbf{I}$ is the unity matrix of size N. Thus, $(\mathbf{H}_k)^{-1} = N^{-1} \cdot \mathbf{H}_k$. This latter property is often employed to define Hadamard matrices of general sizes (e.g. [35]). The *Hadamard transform* $\{\tilde{a}_m\}_{m=0}^{N-1}$ of a sequence $\{a_m\}_{m=0}^{N-1}$ (where $N = 2^k$) is defined as

$$[\tilde{a}_0, \tilde{a}_1, \ldots, \tilde{a}_{N-1}]^T = \mathbf{H}_k \cdot [a_0, a_1, \ldots, a_{N-1}]^T.$$

Now, the main reason that we introduce the Hadamard matrix here, is that it has turned out to be very useful for VQ-description. To see this, consider a general vector valued function $\mathbf{f} : \{0, 1, \ldots, N-1\} \to \mathbb{R}^d$ where the domain is an integer set. Such a function can always be represented as $\mathbf{f}(n) = \mathbf{F} \cdot \mathbf{h}_n, \quad n = 0, 1, \ldots, N-1$, where $\mathbf{h}_n$ is the nth column of an N by N Hadamard matrix $\mathbf{H}$, and $\mathbf{F}$ is a real transform matrix. The matrix $\mathbf{F}$ is obtained as $\mathbf{F} = N^{-1}[\mathbf{f}(0)\ \mathbf{f}(1) \cdots\ \mathbf{f}(N-1)] \cdot \mathbf{H}$. In the special case where $\mathbf{f}$ represents the encoder centroids, $\mathbf{c}_i = E[\mathbf{X}|I = i]$, of a VQ we get the representation, $\mathbf{c}_i = \mathbf{T} \cdot \mathbf{h}_i$. Hence, we obtain an efficient way of describing the mapping from the individual *bits* of the index i to the corresponding encoder centroid. This representation for the encoder centroids is the key to many of the results of the paper. Besides for the representation of VQ centroids the Hadamard representation can be applied to describe the channel signals of the L-dimensional AWGN channel. Given a finite set $\{\mathbf{s}_i\}_{i=0}^{N-1}$ of L-dimensional channel vectors $\mathbf{s}_i$ we can use the Hadamard matrix to express these signals as

$\mathbf{s}_i = \mathbf{K} \cdot \mathbf{h}_i$. This is a useful representation since it gives the relationship between the bits of the index i and the transmitted signal. The received signal $\mathbf{R}$ then becomes $\mathbf{R} = \mathbf{K} \cdot \mathbf{h}_i + \mathbf{W}$ where $\mathbf{W}$ is white and Gaussian.

Appendix B: Proof of Theorem 2

The vector $\hat{\mathbf{p}}(\mathbf{r})$ can be expressed as

$$\begin{aligned}\hat{\mathbf{p}}(\mathbf{r}) &= \frac{\sum_{i=0}^{N-1} \mathbf{h}_i f_{\mathbf{R}|I}(\mathbf{r}|i)}{\sum_{j=0}^{N-1} f_{\mathbf{R}|I}(\mathbf{r}|j)} = \frac{\sum_{i=0}^{N-1} \mathbf{h}_i \exp\left[-(2\sigma_W^2)^{-1}||\mathbf{K}\mathbf{h}_i - \mathbf{r}||^2\right]}{\sum_{j=0}^{N-1} \exp\left[-(2\sigma_W^2)^{-1}||\mathbf{K}\mathbf{h}_j - \mathbf{r}||^2\right]} \\ &= \frac{\sum_{i=0}^{N-1} \mathbf{h}_i \exp\left[-(2\sigma_W^2)^{-1}(2\mathbf{h}_i^T\mathbf{K}^T\mathbf{r} - ||\mathbf{s}_i||^2)\right]}{\sum_{j=0}^{N-1} \exp\left[-(2\sigma_W^2)^{-1}(2\mathbf{h}_j^T\mathbf{K}^T\mathbf{r} - ||\mathbf{s}_j||^2)\right]} = \frac{\sum_{i=0}^{N-1} \mathbf{h}_i \exp\left[-(2\sigma_W^2)^{-1}\mathbf{h}_i^T(2\mathbf{K}^T\mathbf{r} - \mathbf{g})\right]}{\sum_{j=0}^{N-1} \exp\left[-(2\sigma_W^2)^{-1}\mathbf{h}_j^T(2\mathbf{K}^T\mathbf{r} - \mathbf{g})\right]}\end{aligned}$$

where we have canceled common terms and utilized the Hadamard expansions for $\mathbf{s}_i$ and $||\mathbf{s}_i||^2$. Now, consider the function, $\exp\left[-(2\sigma_W^2)^{-1}\mathbf{h}_i^T(2\mathbf{K}^T\mathbf{r} - \mathbf{g})\right]$. It has the form, $\exp(\beta_1 x_1)\exp(\beta_2 x_2)\cdots\exp(\beta_N x_N)$, where $\beta_n \in \{\pm 1\}$. It is straightforward to show that, $\exp(\beta x) = \cosh(x)[1 + \beta\tanh(x)]$, for $\beta \in \{\pm 1\}$ and any real number x. Thus, using the notation $\rho_n = \tanh[r'_n/(2\sigma_W^2)]$, where $r'_n = \{2\mathbf{K}^T\mathbf{r} - \mathbf{g}\}_n$, we have

$$\hat{\mathbf{p}}(\mathbf{r}) = \frac{\sum_{i=0}^{N-1} \mathbf{h}_i(1 + h_0(i)\rho_0)\cdots(1 + h_{N-1}(i)\rho_{N-1})}{\sum_{j=0}^{N-1}(1 + h_0(j)\rho_0)\cdots(1 + h_{N-1}(j)\rho_{N-1})} = \frac{\sum_{i=0}^{N-1} \mathbf{h}_i\tilde{\mathbf{h}}_i^T\mathbf{q}(\mathbf{r})}{\sum_{j=0}^{N-1}\tilde{\mathbf{h}}_j^T\mathbf{q}(\mathbf{r})}$$

where

$$\tilde{\mathbf{h}}_i = \begin{bmatrix}1\\ h_{N-1}(i)\end{bmatrix} \otimes \cdots \otimes \begin{bmatrix}1\\ h_0(i)\end{bmatrix}; \quad \mathbf{q}(\mathbf{r}) = \begin{bmatrix}1\\ \rho_{N-1}\end{bmatrix} \otimes \cdots \otimes \begin{bmatrix}1\\ \rho_0\end{bmatrix}.$$

Noting that $\tilde{\mathbf{h}}_i$ can be written $\tilde{\mathbf{h}}_i = \mathbf{F}\mathbf{h}_i$, $\mathbf{F} \in \mathbb{R}^{2^N \times N}$, we have

$$\hat{\mathbf{p}}(\mathbf{r}) = \frac{\sum_{i=0}^{N-1} \mathbf{h}_i\mathbf{h}_i^T \cdot \mathbf{F}^T\mathbf{q}(\mathbf{r})}{\sum_{j=0}^{N-1} \mathbf{h}_j^T \cdot \mathbf{F}^T\mathbf{q}(\mathbf{r})} = \frac{\mathbf{F}^T\mathbf{q}(\mathbf{r})}{\{\mathbf{F}^T\mathbf{q}(\mathbf{r})\}_0}$$

where we have used that $\sum_{i=0}^{N-1} \mathbf{h}_i\mathbf{h}_i^T = N\mathbf{I}$ and $\sum_{i=0}^{N-1} \mathbf{h}_i^T = N[1, 0, \ldots, 0]$. Since the term $\{\mathbf{F}^T\mathbf{q}(\mathbf{r})\}_0$ is common among the numerator and the denominator in (8) when the expression for $\hat{\mathbf{p}}(\mathbf{r})$ is applied, we have that

$$\hat{\mathbf{h}}(\mathbf{r}) = \frac{\mathbf{R}_{\mathbf{hh}}\mathbf{F}^T\mathbf{q}(\mathbf{r})}{\mathbf{m}_{\mathbf{h}}^T\mathbf{F}^T\mathbf{q}(\mathbf{r})}.$$

Thus, Theorem 2 follows.

Appendix C: Derivation of the Decoding Algorithm

Since $\mathbf{m}_{\mathbf{h}}^T\hat{\mathbf{p}}(\mathbf{r}) = \{\mathbf{f}(\mathbf{r})\}_0$, where $\mathbf{f}(\mathbf{r}) = \mathbf{R}_{\mathbf{hh}}\hat{\mathbf{p}}(\mathbf{r})$, we confine this discussion to the computation of $\mathbf{f} = \mathbf{f}(\mathbf{r})$. Hence, we want to derive an algorithm for the calculation of the vector $\mathbf{f}$ for a VQ having size $N = 2^k$ and index probabilities $\{P_i\}_{i=0}^{N-1}$. Now, let $\mathbf{f}_n(j)$ denote the vector $\mathbf{f}$ for a VQ having arbitrary size $2^n,\ n \le k$, and probabilities $\{P_j, P_{j+1}, \ldots, P_{j+2^n-1}\}$, $j \le 2^k - 2^n$. Also let

$$\mathbf{h}_i^{(n)} = \begin{bmatrix} 1 \\ b_n(i) \end{bmatrix} \otimes \cdots \otimes \begin{bmatrix} 1 \\ b_1(i) \end{bmatrix}; \quad 0 \le i \le 2^n - 1$$

that is, $\mathbf{h}_i^{(n)}$ denotes the ith column of a size 2^n by 2^n Hadamard matrix, and let

$$\hat{\mathbf{p}}^{(n)} = \begin{bmatrix} 1 \\ \hat{b}(r_n) \end{bmatrix} \otimes \cdots \otimes \begin{bmatrix} 1 \\ \hat{b}(r_1) \end{bmatrix}.$$

Then we have

$$\begin{aligned}
\mathbf{f} = \mathbf{f}_k(0) &= \left[\sum_{i=0}^{N-1} P_i \mathbf{h}_i^{(k)} (\mathbf{h}_i^{(k)})^T\right] \hat{\mathbf{p}}^{(k)} \\
&= \left\{\sum_{i=0}^{N-1} P_i \begin{bmatrix} 1 & b_k(i) \\ b_k(i) & 1 \end{bmatrix} \otimes \mathbf{h}_i^{(k-1)} (\mathbf{h}_i^{(k-1)})^T\right\} \left\{\begin{bmatrix} 1 \\ \hat{b}(r_k) \end{bmatrix} \otimes \hat{\mathbf{p}}^{(k-1)}\right\} \\
&= \left\{\sum_{i=0}^{N-1} P_i \begin{bmatrix} 1 & b_k(i) \\ b_k(i) & 1 \end{bmatrix} \begin{bmatrix} 1 \\ \hat{b}(r_k) \end{bmatrix}\right\} \otimes \left\{\mathbf{h}_i^{(k-1)} (\mathbf{h}_i^{(k-1)})^T \hat{\mathbf{p}}^{(k-1)}\right\} \\
&= \begin{bmatrix} 1 + \hat{b}(r_k) \\ \hat{b}(r_k) + 1 \end{bmatrix} \otimes \sum_{i=0}^{N/2-1} P_i \mathbf{h}_i^{(k-1)} (\mathbf{h}_i^{(k-1)})^T \hat{\mathbf{p}}^{(k-1)} + \begin{bmatrix} 1 - \hat{b}(r_k) \\ \hat{b}(r_k) - 1 \end{bmatrix} \otimes \sum_{i=N/2}^{N-1} P_i \mathbf{h}_i^{(k-1)} (\mathbf{h}_i^{(k-1)})^T \hat{\mathbf{p}}^{(k-1)} \\
&= \begin{bmatrix} 1 + \hat{b}(r_k) \\ \hat{b}(r_k) + 1 \end{bmatrix} \otimes \mathbf{f}_{k-1}(0) + \begin{bmatrix} 1 - \hat{b}(r_k) \\ \hat{b}(r_k) - 1 \end{bmatrix} \otimes \mathbf{f}_{k-1}(N/2).
\end{aligned}$$

Consequently, the computation of $\mathbf{f} = \mathbf{f}_k(0)$ can be subdivided into the calculation of $\mathbf{f}_{k-1}(0)$ and $\mathbf{f}_{k-1}(N/2)$. This proves the recursion of (18) (where we used a somewhat different notation). The algorithm is initialized by assigning $\mathbf{f}_0(i) = [P_i],\ i = 0, 1, \ldots, N-1$.

References

[1] C. E. Shannon, "A mathematical theory of communication," *Bell System Technical Journal*, vol. 27, no. 3 and 4, pp. 379–423 and 623–656, July and Oct. 1948.

[2] C. E. Shannon, "Coding theorems for a discrete source with a fidelity criterion," in *IRE National Convention Record*, 1959, pp. 142–163.

[3] J. G. Dunham and R. M. Gray, "Joint source and noisy channel trellis encoding," *IEEE Transactions on Information Theory*, vol. 27, no. 4, pp. 516–519, July 1981.

[4] J. D. Gibson and T. R. Fischer, "Alphabeth-constrained data compression," *IEEE Transactions on Information Theory*, vol. 28, no. 3, pp. 443–457, May 1982.

[5] H. Kumazawa, M. Kasahara, and T. Namekawa, "A construction of vector quantizers for noisy channels," *Electronics and Engineering in Japan*, vol. 67-B, pp. 39–47, Jan. 1984.

[6] E. Ayanoglu and R. M. Gray, "The design of joint source and channel trellis waveform coders," *IEEE Transactions on Information Theory*, vol. 33, no. 6, pp. 855–865, Nov. 1987.

[7] N. Farvardin and V. Vaishampayan, "On the performance and complexity of channel-optimized vector quantizers," *IEEE Transactions on Information Theory*, vol. 37, no. 1, pp. 155–159, Jan. 1991.

[8] K. A. Zeger and A. Gersho, "Zero redundancy channel coding in vector quantization," *IEE Electronics Letters*, vol. 23, no. 12, pp. 654–655, June 1987.

[9] V. Vaishampayan, *Combined source-channel coding for bandlimited waveform channels*, Ph.D. thesis, University of Maryland, College Park, USA, 1989.

[10] V. Vaishampayan and N. Farvardin, "Joint design of block source codes and modulation signal sets," *IEEE Transactions on Information Theory*, vol. 38, no. 4, pp. 1230–1248, July 1992.

[11] N. Phamdo, N. Farvardin, and T. Moriya, "A unified approach to tree-structured and multistage vector quantization for noisy channels," *IEEE Transactions on Information Theory*, vol. 39, no. 3, pp. 835–851, May 1993.

[12] P. Knagenhjelm, *Competitive learning in robust communication*, Ph.D. thesis, Chalmers University of Technology, Göteborg, Sweden, 1993.

[13] F. H. Liu, P. Ho, and V. Cuperman, "Joint source and channel coding using a non-linear receiver," in *Proc. IEEE International Conference on Communications*, Geneva, Switzerland, 1993, pp. 1502–1507.

[14] R. Hagen and P. Hedelin, "Robust vector quantization by a linear mapping of a block code," *IEEE Transactions on Information Theory*, To appear.

[15] P. Hedelin, P. Knagenhjelm, and M. Skoglund, "Vector quantization for speech transmission," in *Speech coding and synthesis*, W. B. Kleijn and K. K. Paliwal, Eds. Elsevier Science, 1995.

[16] P. Hedelin, P. Knagenhjelm, and M. Skoglund, "Theory for transmission of vector quantization data," in *Speech coding and synthesis*, W. B. Kleijn and K. K. Paliwal, Eds. Elsevier Science, 1995.

[17] N. Farvardin, "A study of vector quantization for noisy channels," *IEEE Transactions on Information Theory*, vol. 36, no. 4, pp. 799–809, July 1990.

[18] K. A. Zeger and A. Gersho, "Pseudo-Gray coding," *IEEE Transactions on Communications*, vol. 38, no. 12, pp. 2147–2158, Dec. 1990.

[19] P. Knagenhjelm and E. Agrell, "The Hadamard transform—a tool for index assignment," *IEEE Transactions on Information Theory*, vol. 42, no. 4, pp. 1139–1151, July 1996.

[20] M. Skoglund and P. Hedelin, "Vector quantization over a noisy channel using soft decision decoding," in *Proc. IEEE International Conference on Acoustics, Speech and Signal Processing*, Adelaide, Australia, Apr. 1994, pp. V605–V608.

[21] F. H. Liu, P. Ho, and V. Cuperman, "Joint source and channel coding using a non-linear receiver over Rayleigh fading channel," in *Proc. IEEE Communication Theory Mini-Conference*, Houston, USA, 1993, pp. 1–6.

[22] F. H. Liu, P. Ho, and V. Cuperman, "Sequential reconstruction of vector quantized signals transmitted over Rayleigh fading channels," in *Proc. IEEE International Conference on Communications*, New Orleans, USA, 1994, pp. 23–27.

[23] P. Secker, *Channel-optimised trellis source coding for the memoryless Gaussian channel and applications to spectral parameter coding*, Ph.D. thesis, University of Wollongong, Australia, 1994.

[24] M. Skoglund and P. Hedelin, "A soft decoder vector quantizer for a noisy channel," in *Proc. IEEE International Symposium on Information Theory*, Trondheim, Norway, June 1994, p. 401.

[25] M. Skoglund, "A soft decoder vector quantizer for a Rayleigh fading channel—application to image transmission," in *Proc. IEEE International Conference on Acoustics, Speech and Signal Processing*, Detroit, USA, 1995, pp. 2507–2510.

[26] M. Skoglund and P. Hedelin, "Soft decoding for vector quantization in combination with block channel coding," in *Proc. IEEE International Symposium on Information Theory*, Whistler, Canada, 1995, p. 436.

[27] M. Skoglund, R. Hagen, and P. Hedelin, "Fixed and adaptive decoding in robust LPC quantization," in *Proc. IEEE Speech coding workshop*, Annapolis, USA, 1995, pp. 71–72.

[28] P. Knagenhjelm, "How good is your index assignment?," in *Proc. IEEE International Conference on Acoustics, Speech and Signal Processing*, Minneapolis, USA, Apr. 1993, pp. II:423–426.

[29] R. Hagen and P. Hedelin, "Robust vector quantization by linear mappings of block codes," in *Proc. IEEE International Symposium on Information Theory*, San Antonio, USA, 1993, p. 171.

[30] J. G. Proakis, *Digital Communications*, McGraw-Hill, 3rd edition, 1995.

[31] N. Phamdo and N. Farvardin, "Optimal detection of discrete Markov sources over discrete memoryless channels—applications to combined source-channel coding," *IEEE Transactions on Information Theory*, vol. 40, no. 1, pp. 186–193, Jan. 1994.

[32] A. Gersho and R. M. Gray, *Vector Quantization and Signal Compression*, Kluwer Academic Publishers, 1992.

[33] S. W. McLaughlin, D. L. Neuhoff, and J. J. Ashley, "Optimal binary index assignments for a class of equiprobable scalar and vector quantizers," *IEEE Transactions on Information Theory*, vol. 41, no. 6, pp. 2031–2037, Nov. 1995.

[34] R. M. Gray, *Source Coding Theory*, Kluwer Academic Publishers, 1990.

[35] F. J. MacWilliams and N. J. A. Sloane, *The Theory of Error-Correcting Codes*, North-Holland, Amsterdam, 1977.